Higgs boson exclusive analysis and differential distributions

Dimitris Fassouliotis
University of Athens
On behalf of ATLAS and CMS collaborations

ATLAS EXPERIMENT

National and Kapodistrian University of Athens

CMS Compact Muon Solenoid

Higgs Couplings Workshop 2015, Lumley Castle, 12-15 October

European Union
European Social Fund
OPERATIONAL PROGRAMME
EDUCATION AND LIFELONG LEARNING
investing in knowledge society
MINISTRY OF EDUCATION & RELIGIOUS AFFAIRS
MANAGING AUTHORITY
Co-financed by Greece and the European Union
NSRF 2007-2013
programme for development
EUROPEAN SOCIAL FUND

Contents

- Introduction
- H→ γγ fiducial and differential cross sections
  JHEP09(2014)112 , CMS HIG-14-016, submitted to Eur. Phys. J. C
  ATLAS HIG-15-03, submitted to JHEP
- H→ZZ*→4l fiducial and differential cross sections
  Physics Letters B 738 (2014) 234-253 , CMS PAS HIG-14-028
- Combined γγ and ZZ measurements
  Phys. Rev. Lett. 115 (2015) 091801

Introduction

- **Run I Higgs analysis started as searches**
- **Most analyses reported a signal strength μ, calculated relative to the Standard Model theory prediction**
- **After the discovery of the 125 GeV Higgs boson analyses adapted to measure its properties (mass, width, spin, couplings)**

- **The knowledge of signal kinematics in each production and decay mode allowed to:**

- **use categories and MVAs to discriminate between production modes themselves and backgrounds**
- **search for deviations from the SM in production and decay rates**

However the need to:

- **Describe data in model independent way**
- **Optimize the use of LHC data to constrain Higgs sector and BSM models**
- **Factorize theory uncertainties from experimental ones**

Introduction

Led to :

- **Effective Lagrangian interpretation of measurements**
  (quite complex and with some model assumptions)

- **Fiducial and differential cross section measurements**
  (almost model independent, difficulty to accommodate MVAs)

- **Measurement of differential distributions:**

- **Higgs boson kinematics**
  (sensitive to perturbative QCD modeling and PDFs)
- **Jet activity**
  (sensitive to theoretical modeling and production mechanisms)
- Production sensitive variables
- Lagrangian structure sensitive variables

Introduction: Fiducial differential cross sections

Fiducial cross sections:

- **Minimize model dependence and acceptance corrections**
- **Correct for detector effects for direct comparison with theoretical models**

$$\sigma_i = \frac{v_i^{sig}}{c_i L}$$

Correction factor $c_i = \frac{N_i^{reco}}{N_i^{fid}}$

Where i corresponds to the i bin of a differential distribution

- **Baseline fiducial cross section can be considered as single bin**

- **Instead of the correction factor, the full response matrix can be used**

$$N_i^{reco} = L \cdot \sum_j \left(M_{ij} \sigma_j \right)$$

and perform simultaneously unfolding and signal extraction (CMS method) or use iterative Bayesian unfolding (ATLAS cross check method)

- Providing that possible biases of the bin-by-bin method are properly accounted for by systematic uncertainties both methods are valid
- Difference is minimal for distributions with low migrations

Introduction: MC simulation

At E_{cm}=8 TeV and m_H ~125 GeV:

ggF 87.3%, VBF 7.1%, WH 3.1%, ZH 1.9%, ttH 0.6%

Most studies target measurements for **ggF** production

Inclusive ggF cross section calculations		
LHC-XS	NNLO+NNLL	CERN-2011-002(2011), arXiv1101.0593
ADDFGHLM	N^3LO	J. High Energy Phys. 12 (2011) 058 - arXiv1503.6056
ABNY	NNLO+NNLL	Phys. Lett. B 698 (2011) 271-274, arXiv1008.3162
STWZ	NNLO	Phys. Rev. D 89 (2014) 054001, arXiv1307.1808
dFMMV	approx. N^3LO	J. High Energy Phys. 10 (2014) 176, arXiv1408.6227
BBFMR	approx. N^3LO+N^3LL	J. High Energy Phys. 09 (2014) 007, arXiv1405.3654

Differences, special characteristics on back-up slides

Inclusive cross section calculations for additional production mechanisms

VBF : NNLO in QCD, NLO in EW

VH : NNLO in QCD, NLO in EW

ttH : NLO in QCD, LO in EW

Introduction: MC simulation

Analytical ggF differential cross section predictions		
HRES 2.2	NNLO+NNLL	J. High Energy Phys. 09 (2013) 129, arXiv1306.4581
STWZ, BLPTW	NNLO+NNLL	Phys. Rev. D 89 (2014) 074044, arXiv1312.4535
JetVHeto 2.0	NNLO+NNLL	J. High Energy Phys. 01 (2014) 097, arXiv1308.4634

Monte Carlo ggF event generators		
SHERPA 2.1.1	H+0,1,2 jets @NLO	Phys. Rev. D 90 (2014) 014012, arXiv1401.7971
MG5_aMC@NLO	H+0,1,2 jets @NLO	J. High Energy Phys. 07 (2014) 079, arXiv1405.0301
POWHEG NNLOPS	NNLO ≥0 jet, NLO ≥ 1 jet	J. High Energy Phys. 10 (2013) 222, arXiv1309.0017

Differences, special characteristics on back-up slides

Monte Carlo generators for additional production mechanisms

VBF : POWHEG, NLO

VH, ttH : PYTHIA, LO

H→ γγ fiducial differential cross sections

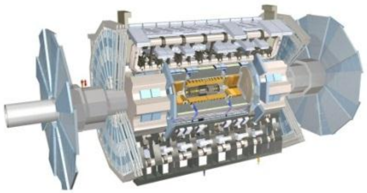

Simulated samples

- POWHEG, MINLO, SHERPA 1.4.3 with 0-4jets
- PYTHIA8, HERWIG with or w/o MPI

Analysis – Fiducial phase space

$|\eta_\gamma|<2.37$ (excluding $1.37<|\eta_\gamma|<1.56$), $p_{T\gamma1} > 0.35 m_{\gamma\gamma}$, $p_{T\gamma2} > 0.25 m_{\gamma\gamma}$, $E_T^{iso(\Delta R=0.4)} < 14$ GeV

Jets: Anti-kt with R=0.4, p_T>30 GeV, $|\eta|<4.4$, JFV>0.25 (for jets with p_T<50 GeV)

- ➢ Simultaneous unbinned ML fit in each observable to extract signal. m_H=125.4 GeV
- ➢ Correction factor for baseline fiducial 0.66

Fiducial cross section measurements:

Baseline, N_{jets}, $N_{leptons}$, E_t^{mis} and VBF-enhanced

$$\sigma_i = \frac{\nu_i^{sig}}{c_i L}$$

Systematic uncertainties:

- ➢ Signal extraction
- ➢ Luminosity
- ➢ Correction factor
- Exp. uncertainties
- Theoretical modeling

Source	Uncertainty on fiducial cross section (%)				
	Baseline	$N_{jets} \geq 1$	$N_{jets} \geq 2$	$N_{jets} \geq 3$	VBF-enhanced
Signal extraction (stat.)	±22	±25	±30	±33	±34
Signal extraction (syst.)	±6.5	±7.4	±7.1	±6.5	±9.0
Photon efficiency	±1.5	±2.1	±3.1	±4.2	±2.3
Jet energy scale/resolution	-	$^{+6.2}_{-5.8}$	$^{+11}_{-10}$	$^{+15}_{-13}$	$^{+12}_{-11}$
JVF/pileup-jet	-	±1.3	±2.2	±3.3	±0.5
Theoretical modelling	$^{+3.3}_{-1.0}$	$^{+5.0}_{-2.6}$	±4.1	$^{+6.3}_{-4.9}$	$^{+2.2}_{-3.2}$
Luminosity	±2.8	±2.8	±2.8	±2.8	±2.8

H→ γγ fiducial cross section

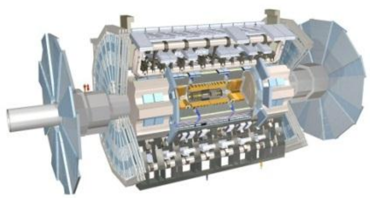

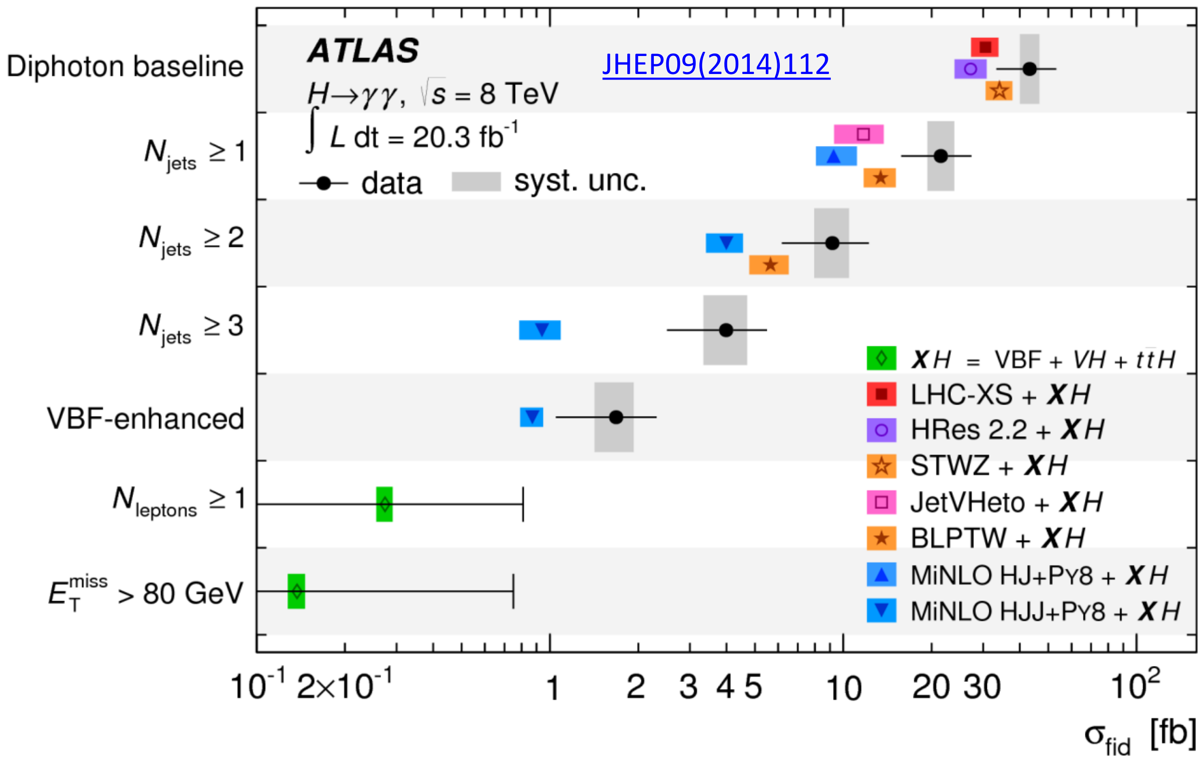

HRes2.2
lower prediction than LHC-XS

- missing EW corrections
- threshold resummation
- Use of different PDF

STWZ
higher prediction than LHC-XS
despite missing EW corrections

Higher order of
BLPTW and JetVHeto
w.r.t. MINLO
seem important

$$\sigma^{fid}_{obs}(pp \rightarrow H \rightarrow \gamma\gamma) = 43.2 \pm 9.4(stat)^{+3.2}_{-2.9}(syst) \pm 1.2(lumi)\ fb$$

$$\sigma^{fid}_{th} = 30.5 \pm 3.3$$ (LHC-XS)

$$\frac{\sigma_{fid}}{\sigma_{th}} = 1.41 \pm 0.36$$

Consistent with dedicated signal strength measurement

H→ γγ fiducial differential cross sections

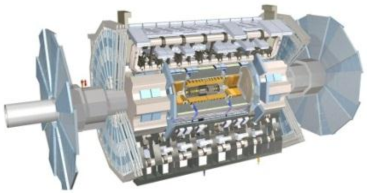

Differential distributions:

P_T^H, $|y^H|$, $|\cos\vartheta^*|$, N_{jets}, H_T, P_T^{J1}, P_T^{J2}, y^{J1}, $\Delta\varphi^{JJ}$, Δy^{jj}, $\Delta\varphi^{H\text{-}JJ}$

P_T^H JHEP09(2014)112

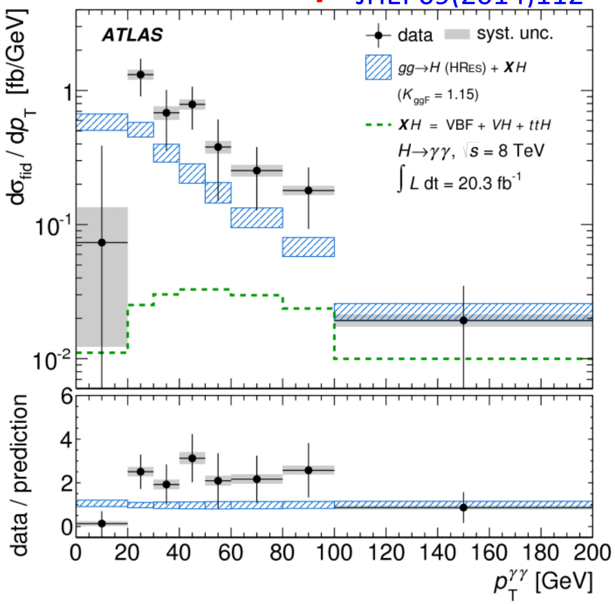

y^H JHEP09(2014)112

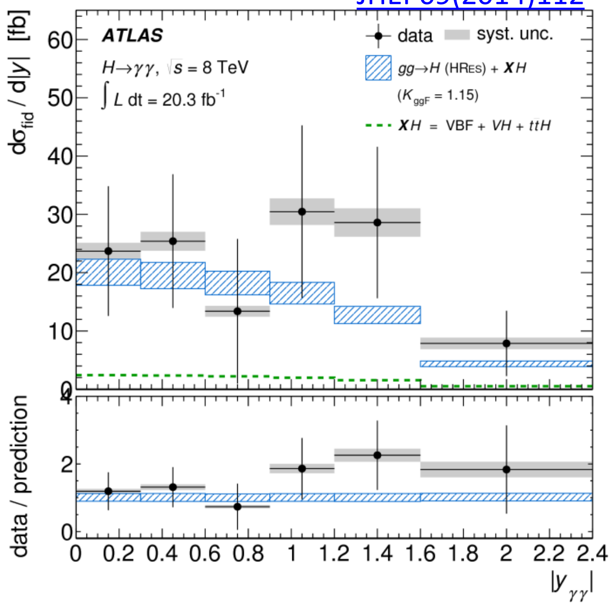

N_{jets} JHEP09(2014)112

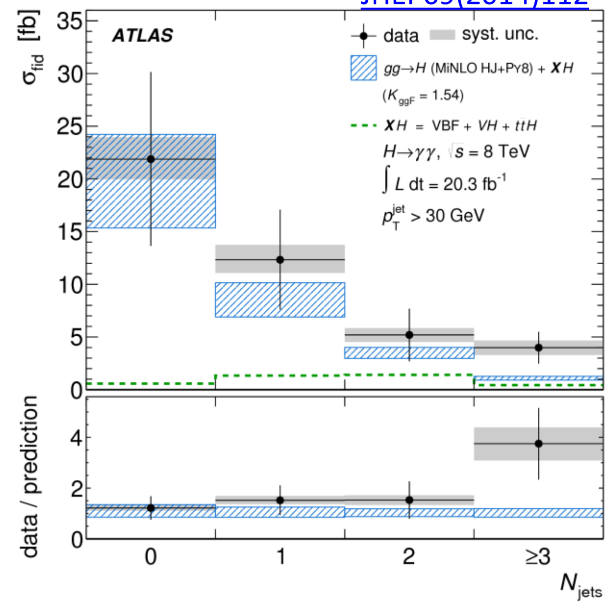

H→ γγ fiducial differential cross sections

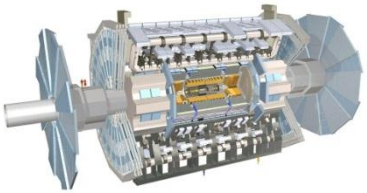

P_T^{J1} JHEP09(2014)112

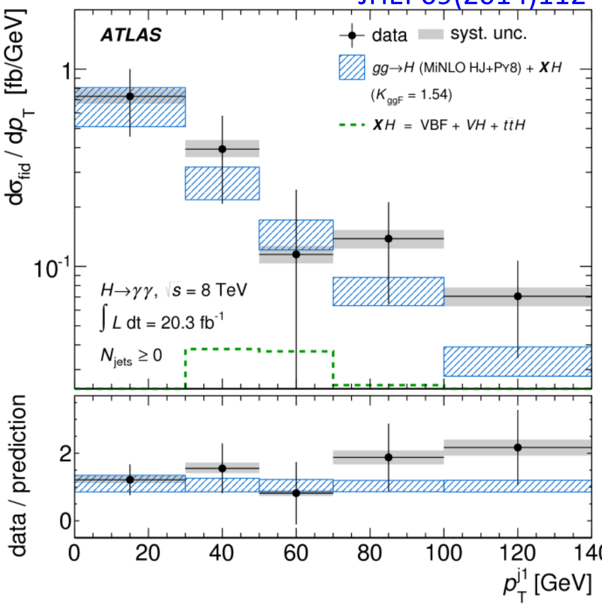

P_T^{J2} JHEP09(2014)112

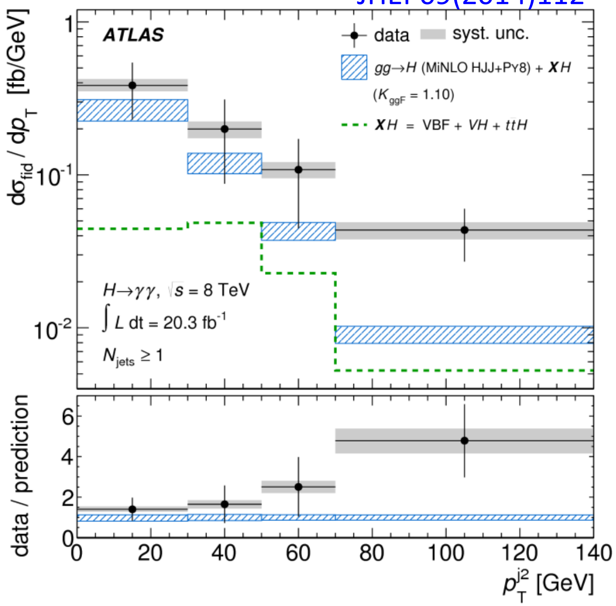

$\Delta\varphi^{jj}$ JHEP09(2014)112

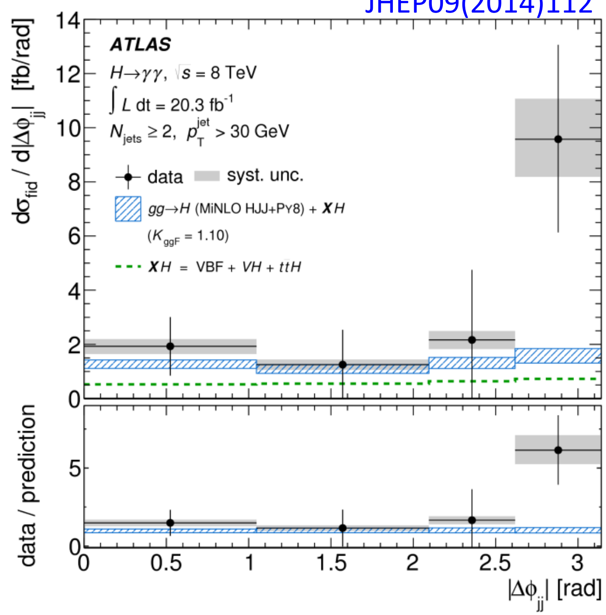

The increased jet activity and harder jet spectra, could suggest the presence of higher quark and gluon radiation in the data than in the theoretical predictions

Deviation in **$\Delta\phi_{jj}$** of 2.3σ (local p-value)
Stable with central jets with stronger JVF criteria → pile-up not responsible
Also double parton scattering ~ 1.3%

H→ γγ differential distributions – EFT interpretation

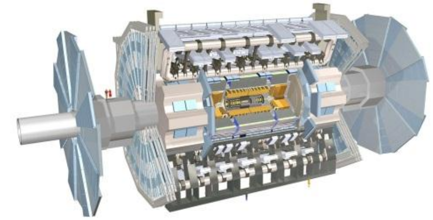

ATLAS HIG-15-03, submitted to JHEP

E L framework implemented with FeynRules+MADGRAPH5

$$\mathcal{L} = \bar{c}_\gamma O_\gamma + \bar{c}_g O_g + \bar{c}_{HW} O_{HW} + \bar{c}_{HB} O_{HB} + \tilde{c}_\gamma \tilde{O}_\gamma + \tilde{c}_g \tilde{O}_g + \tilde{c}_{HW} \tilde{O}_{HW} + \tilde{c}_{HB} \tilde{O}_{HB},$$

Simultaneous fit on differential distributions: P_T^H, N_{jets}, P_T^{J1}, $\Delta\varphi^{JJ}$, m^{jj}

Statistical correlations between differential distributions were estimated using the bootstrap method

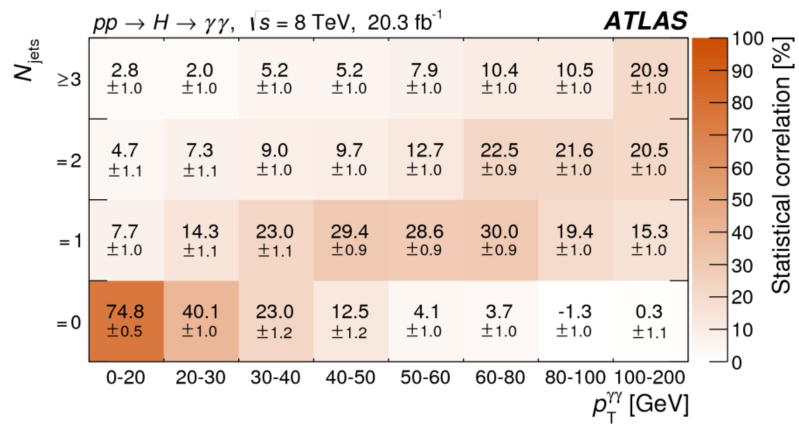

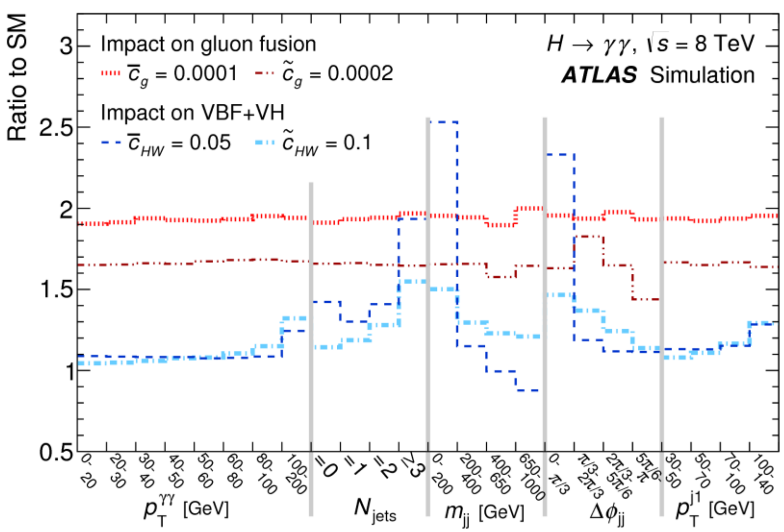

Coefficient	95% 1 − CL limit
$\bar{c}_\gamma$	$[-7.4,\ 5.7]\times10^{-4} \cup [3.8,\ 5.1]\times10^{-3}$
$\tilde{c}_\gamma$	$[-1.8,\ 1.8]\times10^{-3}$
$\bar{c}_g$	$[-0.7,\ 1.3]\times10^{-4} \cup [-5.8,\ -3.8]\times10^{-4}$
$\tilde{c}_g$	$[-2.4,\ 2.4]\times10^{-4}$
$\bar{c}_{HW}$	$[-8.6,\ 9.2]\times10^{-2}$
$\tilde{c}_{HW}$	$[-0.23,\ 0.23]$

All compatible with SM, where c_x=0

H→ γγ fiducial differential cross sections

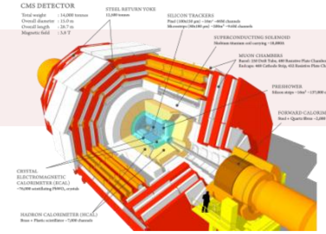

CMS HIG-14-016, submitted to Eur. Phys. J. C

Simulated samples

- POWHEG, JHU - PYTHIA6.4

Analysis – Fiducial phase space

$|\eta_\gamma|<2.5$ (excluding $1.44<|\eta_\gamma|<1.57$), $p_{T\gamma1}>0.33m_{\gamma\gamma}$, $p_{T\gamma2}>0.25m_{\gamma\gamma}$, $E_T^{iso(\Delta R=0.4)}<10$ GeV

Jets: Anti-kt with R=0.5, p_T>25 GeV, $|\eta|<4.7$, anti pile-up criteria

-at least one jet required with $|\eta|<2.5$ for N_{jets} and leading jet studies-

- Three $m_{\gamma\gamma}$ resolution classes
- Simultaneous binned ML fit in all bins of each observable. Variable m_H
- Unfolding performed together with signal extraction in the ML fit

Systematic Uncertainties (a difference)

Uncertainty of signal events from associated production using ±50% of SM values, contrary to ATLAS analysis estimated from 0.5-2x (VBF and VH), 0-5x (ttH) SM values

$$\sigma^{fid}_{obs}(pp \to H \to \gamma\gamma) = 32^{+10}_{-10}(stat)^{+3}_{-3}(syst)\ fb$$

$$\sigma^{fid}_{th}(HRES + XH) = 31^{+4}_{-3}\ fb$$

$$\sigma^{fid}_{th}(POWHEG + XH) = 32^{+6}_{-5}\ fb$$

$$\sigma^{fid}_{th}(MADGRAPH5\_aMC@NLO + XH) = 30^{+6}_{-5}\ fb$$

All MC estimations are scaled to reproduce LHC-XS inclusive cross section

H→ γγ fiducial differential cross sections

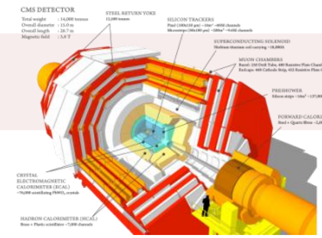

Differential distributions:

P_T^H, $|y^H|$, $|cos\vartheta^*|$, $\Delta\varphi^{\gamma\gamma}$, N_{jets}, m_{jj}, P_T^{J1}, $|y^H\text{-}y^{J1}|$, $\Delta\varphi^{JJ}$, $\Delta\eta^{jj}$, $\Delta\varphi^{H\text{-}JJ}$

P_T^H

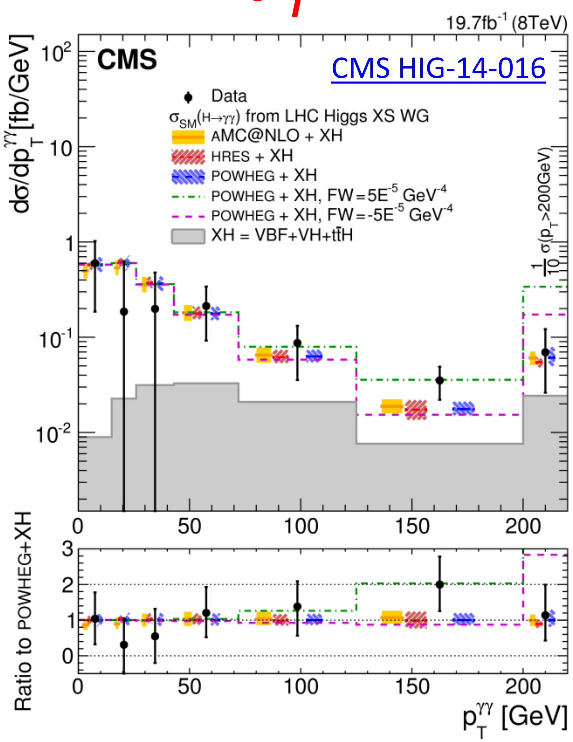

y^H

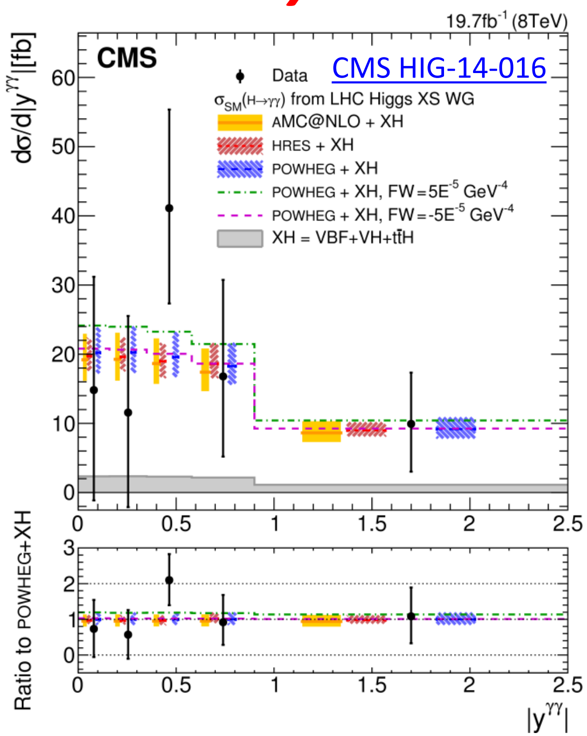

N_{jets}

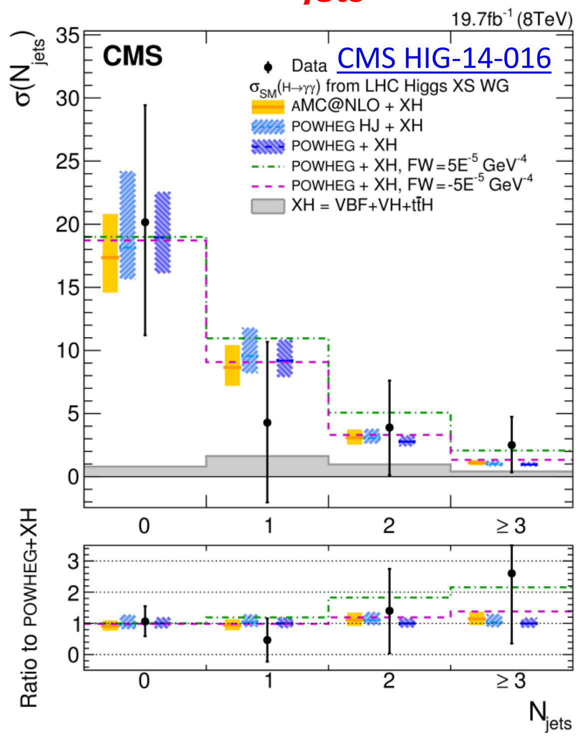

Last bin includes the over-flow of each distribution

H→ γγ fiducial differential cross sections

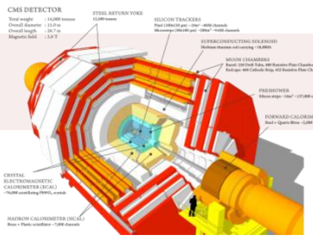

P_T^{J1}

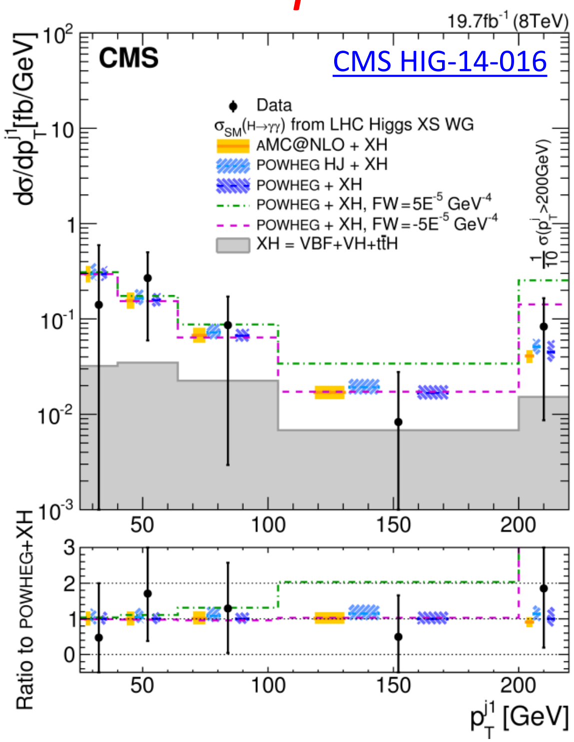

$\Delta\eta^{jj}$

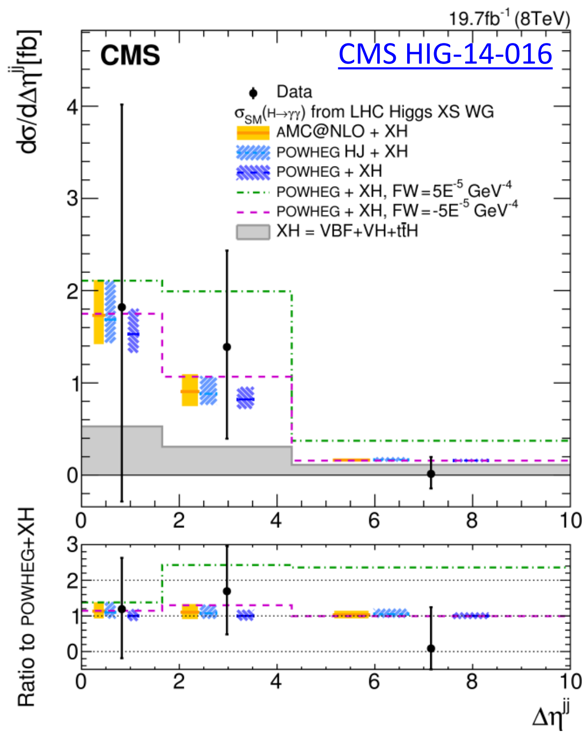

$\Delta\varphi^{jj}$

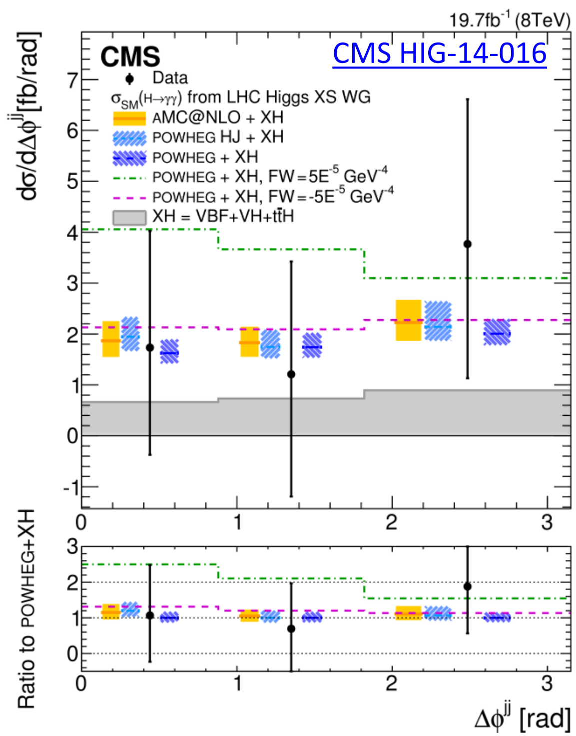

No direct comparison with ATLAS results on jet activity and p_T spectra, due to differences in the definition of the fiducial volume.

No significant deviation from theoretical predictions is observed.

H→ ZZ(*)→4l fiducial differential cross sections

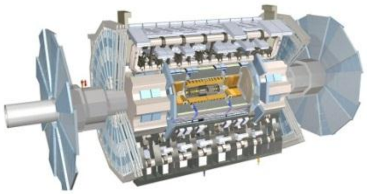

Simulated samples

- POWHEG, MINLO, JHU - PYTHIA8

Analysis

Similar to the one used for the signal strengths. m_H=125.4 GeV

➢ Correction factor for baseline fiducial 0.55

Fiducial phase space requirements

Lepton selection	
Muons:	$p_T > 6$ GeV, $\lvert\eta\rvert < 2.7$
Electrons:	$p_T > 7$ GeV, $\lvert\eta\rvert < 2.47$
Lepton pairing	
Leading pair:	SFOS lepton pair with smallest $\lvert m_Z - m_{\ell\ell}\rvert$
Subleading pair:	Remaining SFOS lepton pair with smallest $\lvert m_Z - m_{\ell\ell}\rvert$
Event selection	
Lepton kinematics:	$p_T > 20, 15, 10$ GeV
Mass requirements:	$50 < m_{12} < 106$ GeV
	$12 < m_{34} < 115$ GeV
Lepton separation:	$\Delta R(\ell_i, \ell_j) > 0.1$ (0.2) for same- (different-) flavour leptons
J/ψ veto:	$m(\ell_i, \ell_j) > 5$ GeV for all SFOS lepton pairs
Mass window:	$118 < m_{4\ell} < 129$ GeV

Systematic Uncertainties (%)	
Background	
Luminosity	1.4–2.3
Reducible background	1.6–34
Experimental, leptons	1.3–2.3
PDF/scale	3.0–24
Correction factors/conversion to σ	
Luminosity	2.8
Experimental, leptons	2.1–2.6
Experimental, jets	2.7–13
Production process	0.1–15
Higgs boson mass	0.4–2.7

$$\sigma^{\text{fid}}_{\text{obs}} = 2.11^{+0.53}_{-0.47}(\text{stat}) \pm 0.08(\text{syst})\ \text{fb}$$

$$\sigma^{\text{fid}}_{\text{th}} = 1.30 \pm 0.13\ \text{fb}$$ (LHC-XS)

H→ ZZ(*)→4l fiducial differential cross sections

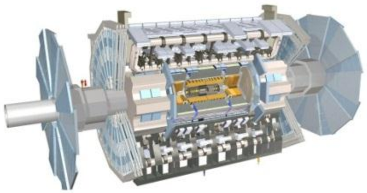

Differential distributions:

P_T^H, $|y^H|$, m_{34}, $|cos\vartheta^*|$, N_{jets}, P_T^{J1}

In the differential distribution bins
Signal estimation →Observed events - Background

Physics Letters B 738 (2014) 234-253

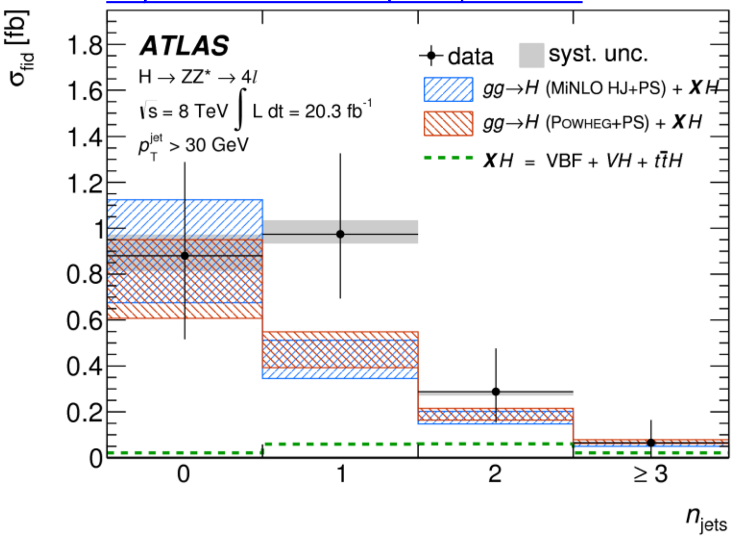

Variable	POWHEG	p-values MINLO	HRES2
$p_{T,H}$	0.30	0.23	0.16
$\|y_H\|$	0.37	0.45	0.36
m_{34}	0.48	0.60	-
$\|\cos\theta^*\|$	0.35	0.45	-
n_{jets}	0.37	0.28	-
$p_{T,jet}$	0.33	0.26	-

Physics Letters B 738 (2014) 234-253

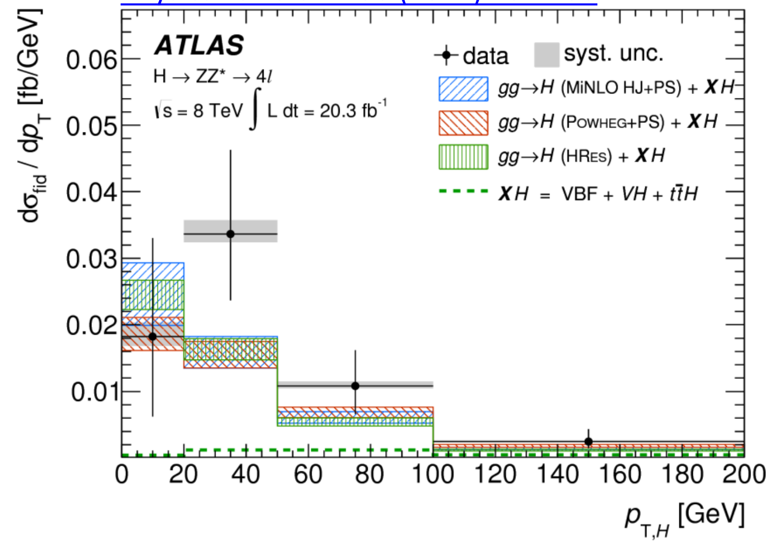

Physics Letters B 738 (2014) 234-253

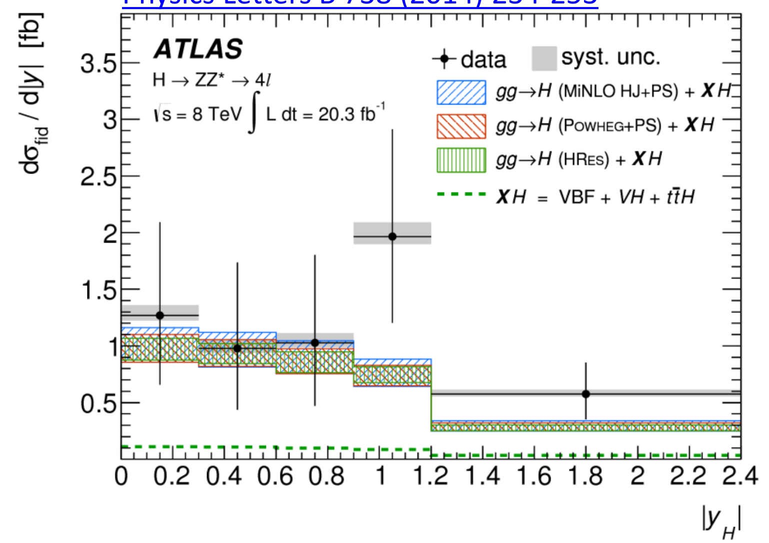

H→ ZZ(*)→4l fiducial differential cross sections

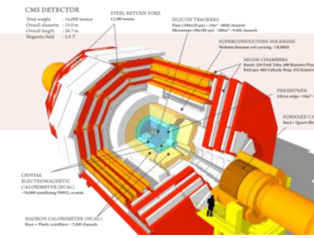

Simulated samples

- POWHEG, MINLO, JHU - PYTHIA6.4

Analysis

Similar to the one used for the signal strengths

m_H=125.0 GeV

- Correction factor for baseline fiducial 0.65

Requirements for the $H \to 4\ell$ fiducial phase space	
Lepton kinematics and isolation	
leading lepton p_T	$p_T > 20$ GeV
next-to-leading lepton p_T	$p_T > 10$ GeV
additional electrons (muons) p_T	$p_T > 7(5)$ GeV
pseudorapidity of electrons (muons)	$\|\eta\| < 2.5(2.4)$
p_T sum of all stable particles within $\Delta R < 0.4$ from lepton	less than $0.4 \cdot p_T$
Event topology	
existence of at least two SFOS lepton pairs, where leptons satisfy criteria above	
inv. mass of the Z_1 candidate	$40\,\text{GeV} < m(Z_1) < 120\,\text{GeV}$
inv. mass of the Z_2 candidate	$12\,\text{GeV} < m(Z_2) < 120\,\text{GeV}$
distance between selected four leptons	$\Delta R(\ell_i \ell_j) > 0.02$ for any $i \neq j$
inv. mass of any opposite sign lepton pair	$m(\ell^+ \ell'^-) > 4\,\text{GeV}$
inv. mass of the selected four leptons	$105\,\text{GeV} < m_{4\ell} < 140\,\text{GeV}$
the selected four leptons must originate from the $H \to 4\ell$ decay	

- Signal model with non-resonant part (WH,ZH,ttH)
- Procedure applied also on Z→4l

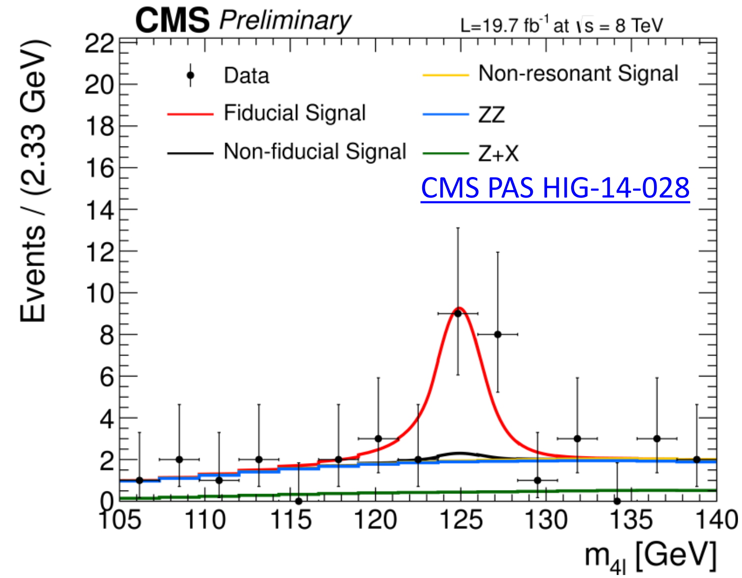

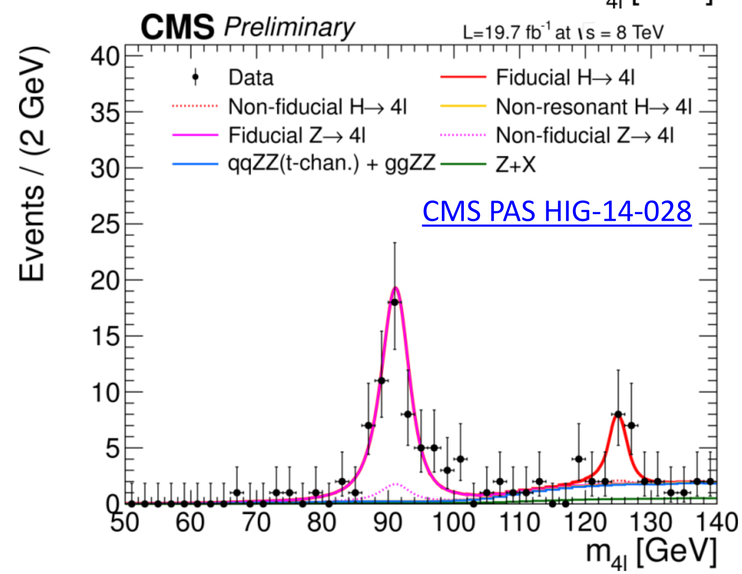

H→ ZZ(*)→4l fiducial differential cross sections

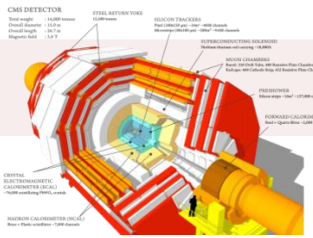

Systematic Uncertainties

- Experimental leptons 4-10%
- Experimental jets 3-12%
- Irreducible bkg qq: 4.5, gg:25%
- Reducible bkg 20-40%
- Theory Modeling 1 (7)%, 3-5 (25)%
- Mass 1%
- Luminosity 2.6%

Fiducial cross section $H \to 4\ell$ at 7 TeV	
Measured	$0.56^{+0.67}_{-0.44}$ (stat.) $^{+0.21}_{-0.06}$ (sys.) $^{+0.02}_{-0.02}$ (model) fb
$gg \to$ H(HRES) + XH	$0.93^{+0.10}_{-0.11}$ fb
Fiducial cross section $H \to 4\ell$ at 8 TeV	
Measured	$1.11^{+0.41}_{-0.35}$ (stat.) $^{+0.14}_{-0.10}$ (sys.) $^{+0.08}_{-0.02}$ (model) fb
$gg \to$ H(HRES) + XH	$1.15^{+0.12}_{-0.13}$ fb
Ratio of fiducial cross sections of $H \to 4\ell$ at 7 and 8 TeV	
Measured	$0.51^{+0.71}_{-0.40}$ (stat.) $^{+0.13}_{-0.05}$ (sys.) $^{+0.00}_{-0.03}$ (model)
$gg \to$ H(HRES) + XH	$0.805^{+0.003}_{-0.010}$

Fiducial cross section $Z \to 4\ell$ at 8 TeV ($50\,\mathrm{GeV} < m_{4\ell} < 105\,\mathrm{GeV}$)	
Measured	$4.81^{+0.69}_{-0.63}$(stat.)$^{+0.18}_{-0.19}$(sys.) fb
POWHEG	$4.56^{+0.19}_{-0.19}$ fb
Ratio of fiducial cross sections of $H \to 4\ell$ and $Z \to 4\ell$ at 8 TeV ($50\,\mathrm{GeV} < m_{4\ell} < 140\,\mathrm{GeV}$)	
Measured	$0.21^{+0.09}_{-0.07}$(stat.)$^{+0.01}_{-0.01}$(sys.)
$gg \to$ H(HRES) + XH and $Z \to 4\ell$ (POWHEG)	$0.25^{+0.04}_{-0.04}$

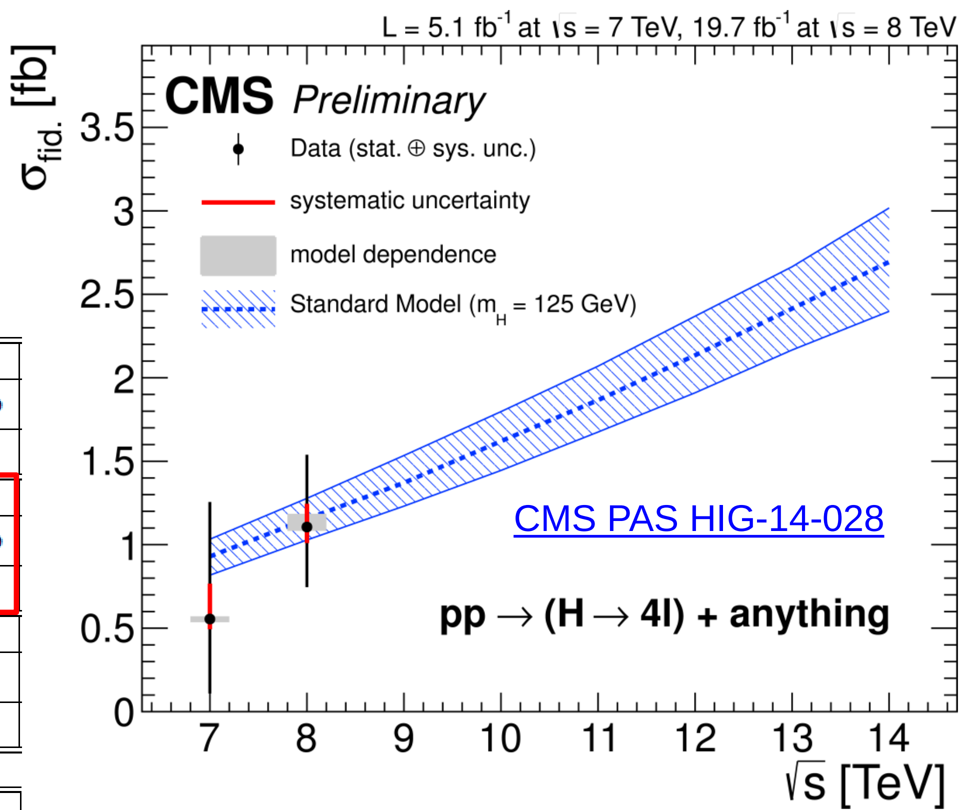

H→ ZZ(*)→4l fiducial differential cross sections

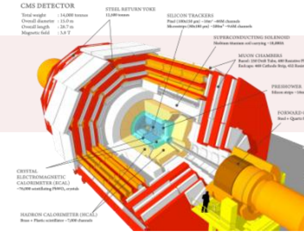

Differential distributions: P_T^H, $|y^H|$, N_{jets}, P_T^{J1}, $|y^H\text{-}y^{J1}|$

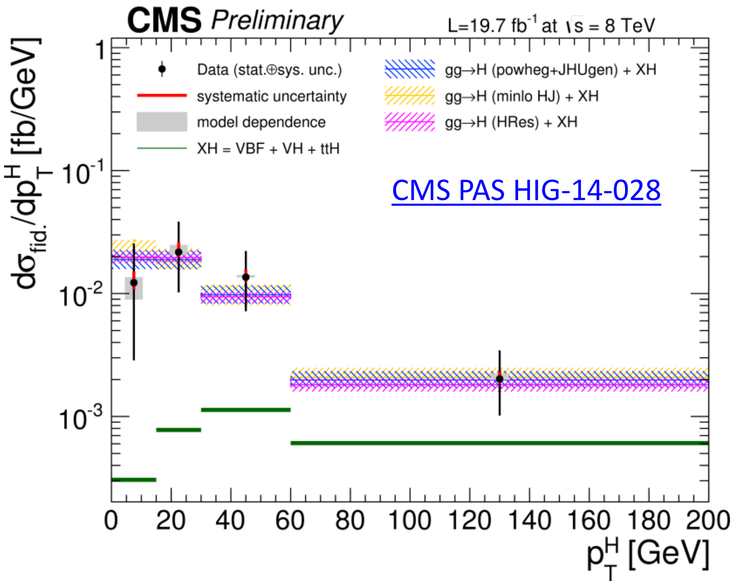

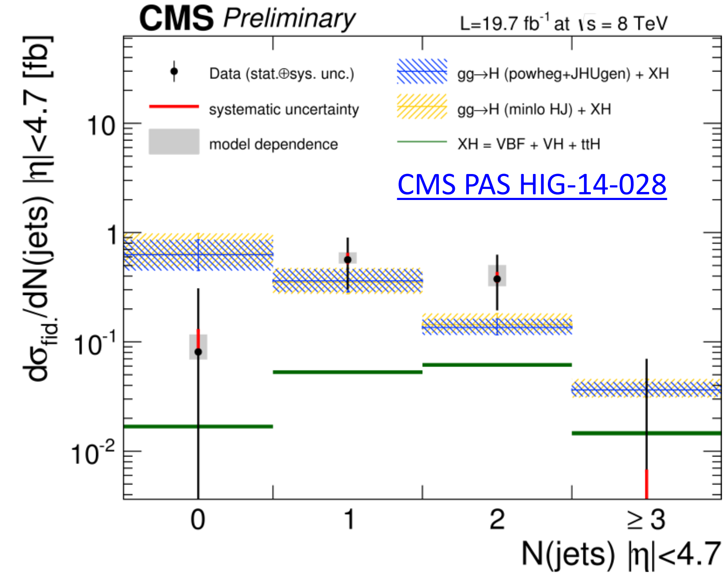

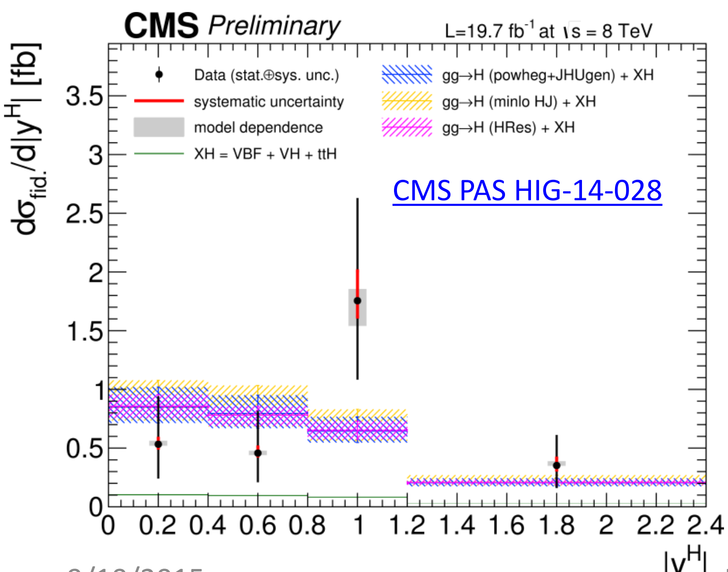

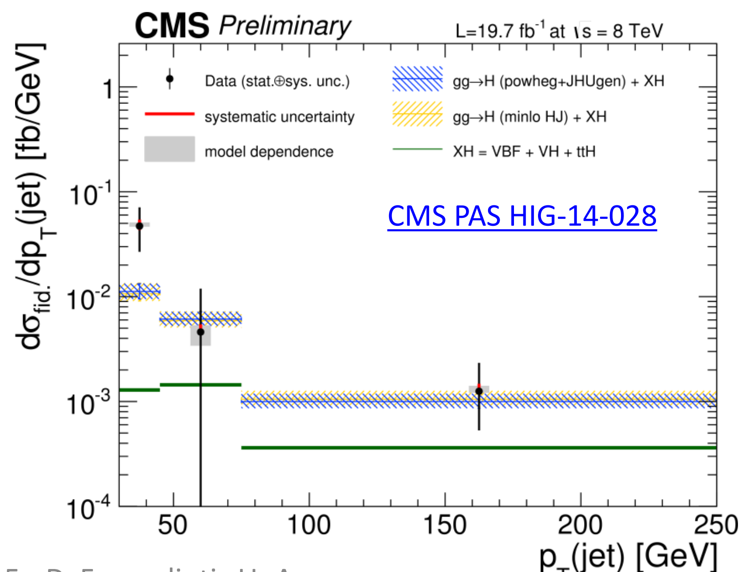

Combined γγ ZZ fiducial differential cross sections

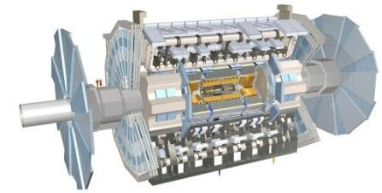

- Combination improves results by 25-40%
- Differential distributions ***P_T^H , $|y^H|$, N_{jets} , P_T^{J1}***
- Fiducial acceptance: H→γγ 56-62%, H→ZZ→4l 44-53%
- m_H= 125.36±0.41 GeV (measured by ATLAS), Br(H→γγ)=0.228%, Br(H→ZZ*→4l)=0.0129%
- Good agreement between channels
- Same uncertainty sources treated as fully correlated
- Statistical uncertainties still dominant

Total cross section measurement

$$\sigma(pp \to H) = 33.0 \pm 5.3(\mathrm{stat}) \pm 1.6(\mathrm{syst})\ \mathrm{pb}$$

$$\sigma_i = \frac{v_i^{sig}}{B\alpha_i c_i L}$$

Acceptance

Branching ratio

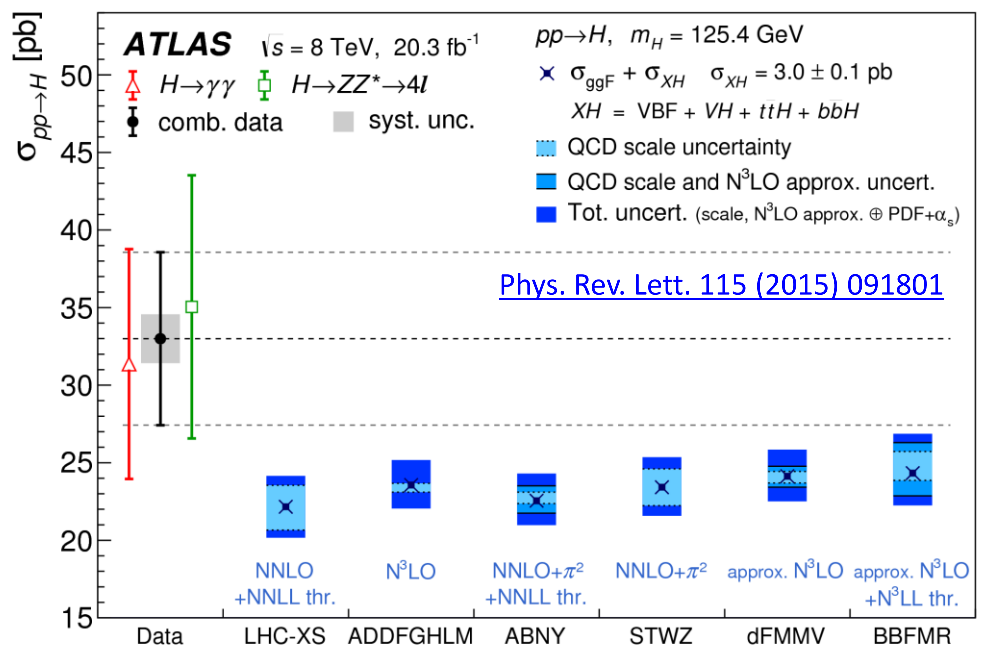

Combined γγ ZZ fiducial differential cross sections

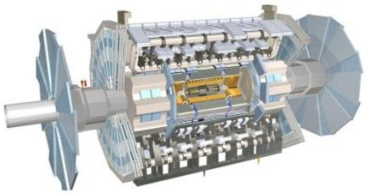

[Phys. Rev. Lett. 115 (2015) 091801](#)

Measured Higgs boson production cross sections in inclusive and exclusive jet multiplicity bins compared to different theoretical predictions

- NLO-accurate multi-leg merged generators are used
- For N_{jets}≥1 MC predictions and analytical calculations have NLO accuracy
- Poorest agreement in inclusive and exclusive 1-jet bins with p-values ranging between 0.1% and 3.6%

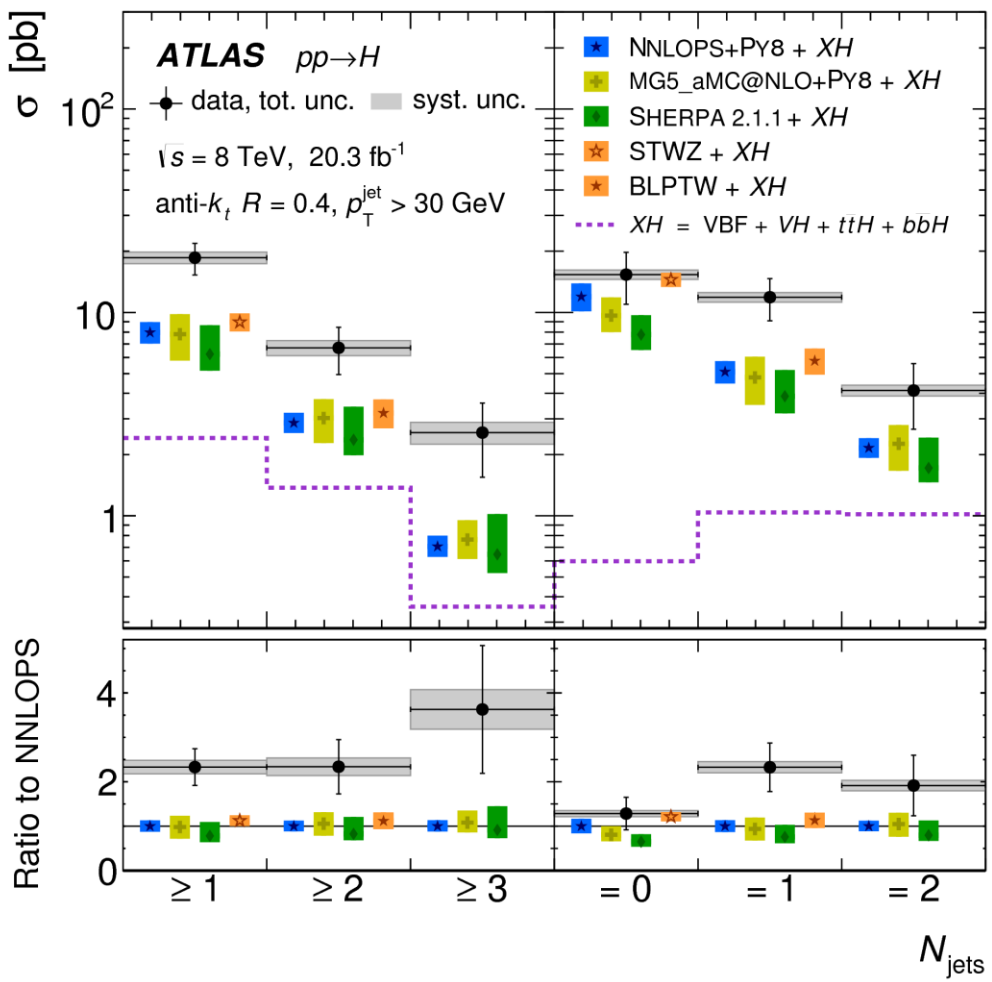

Combined γγ ZZ fiducial differential cross sections

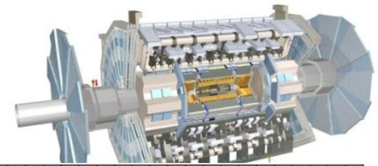

Phys. Rev. Lett. 115 (2015) 091801

differential cross-sections

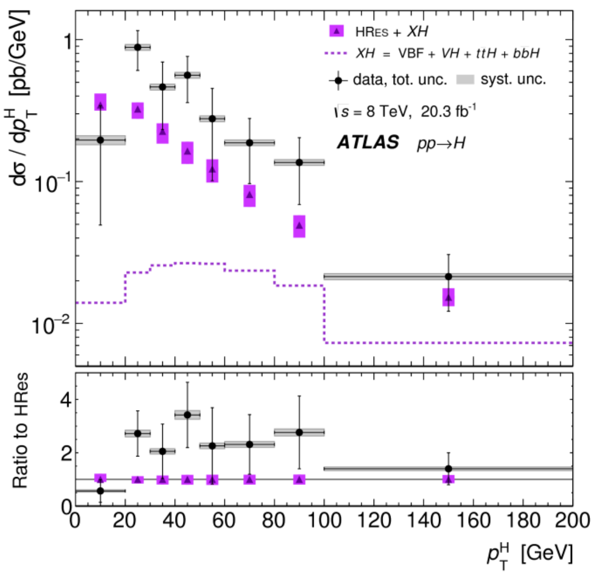

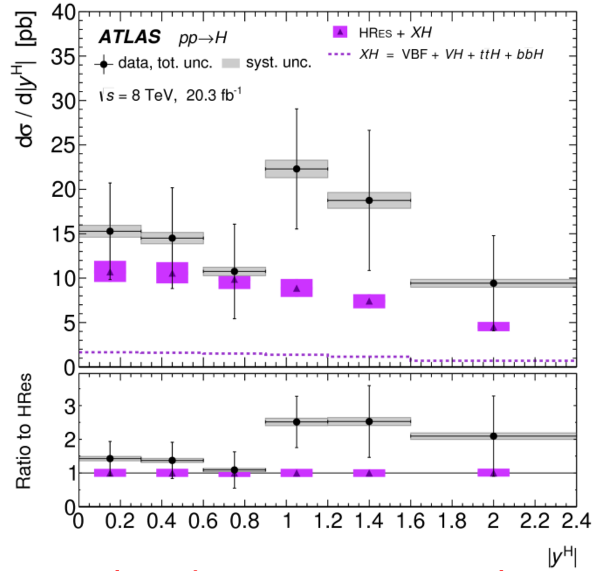

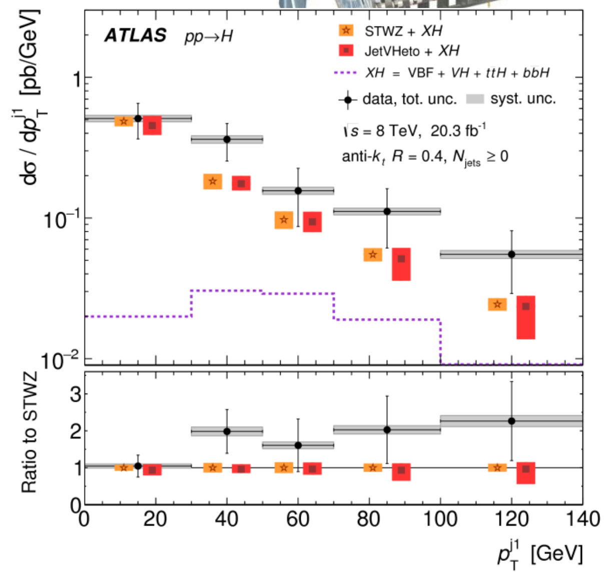

normalized cross-section shapes

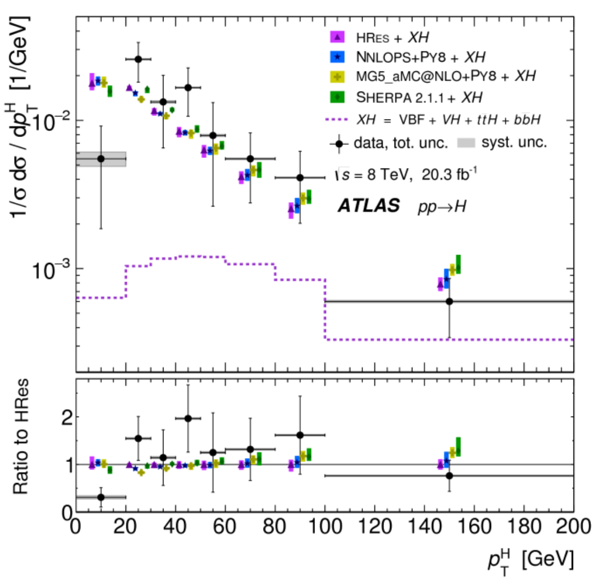

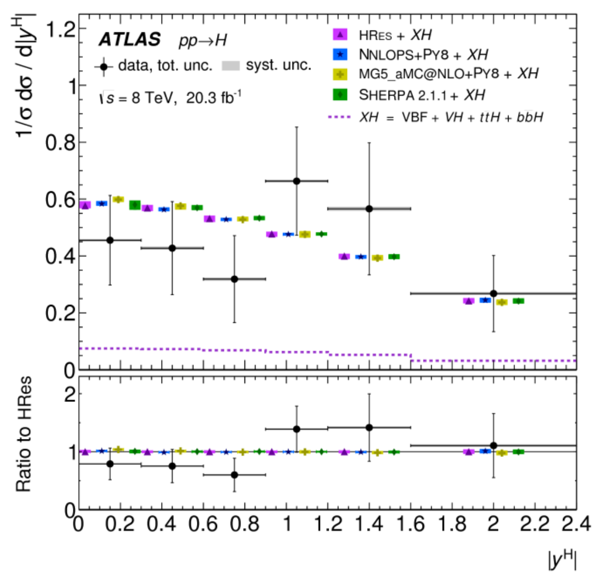

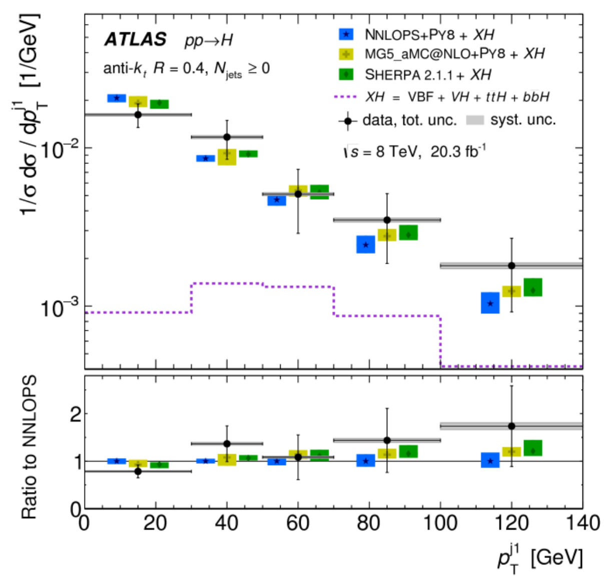

Summary

- With RUN I data, **several measurements of fiducial cross sections** have been performed by ATLAS and CMS.
- Also, several **differential distributions** concerning Higgs boson kinematics, and jet activity produced in association with the Higgs boson have been studied.

- Systematic uncertainties are similar between the two experiments.
- ATLAS $H\rightarrow\gamma\gamma$ analysis shows hints for higher jet activity than expected from theoretical models, having also a deviation towards back-to back jet production, but this not supported by CMS $H\rightarrow\gamma\gamma$ analysis.
- Both report a small deviation in the rapidity spectrum of the Higgs boson in the $H\rightarrow ZZ^*\rightarrow 4l$ channels, but this is not seen in either of the $H\rightarrow\gamma\gamma$ analysis.

- In total, **no significant disagreement with the SM is observed.**
- **All measurements are dominated by statistical errors** -and therefore-
- Run II offers great opportunities for precision measurements on the Higgs sector

- LHC Higgs WG initiated (June 2015) a fiducial cross section task force

Back-up slides

Back-up slides

This research has been co-financed by the European Union (European Social Fund - ESF) and Greek national funds through the Operational Program "Education and Lifelong Learning" of the National Strategic Reference Framework (NSRF) - Research Funding Program: THALES. Investing in knowledge society through the European Social Fund.

H→ γγ fiducial differential cross sections

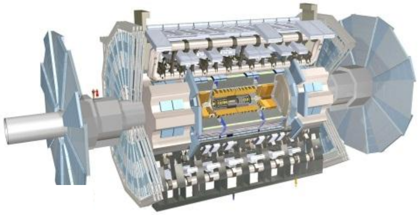

JHEP09(2014)112

Fiducial region	Measured cross section (fb)
Baseline	$43.2 \pm 9.4\,(\text{stat.})\,^{+3.2}_{-2.9}\,(\text{syst.}) \pm 1.2\,(\text{lumi})$
$N_{\text{jets}} \geq 1$	$21.5 \pm 5.3\,(\text{stat.})\,^{+2.4}_{-2.2}\,(\text{syst.}) \pm 0.6\,(\text{lumi})$
$N_{\text{jets}} \geq 2$	$9.2 \pm 2.8\,(\text{stat.})^{+1.3}_{-1.2}\,(\text{syst.}) \pm 0.3\,(\text{lumi})$
$N_{\text{jets}} \geq 3$	$4.0 \pm 1.3\,(\text{stat.}) \pm 0.7\,(\text{syst.}) \pm 0.1\,(\text{lumi})$
VBF-enhanced	$1.68 \pm 0.58\,(\text{stat.})^{+0.24}_{-0.25}\,(\text{syst.}) \pm 0.05\,(\text{lumi})$
$N_{\text{leptons}} \geq 1$	< 0.80
$E_{\text{T}}^{\text{miss}} > 80$ GeV	< 0.74

Table 3. Measured cross sections in the baseline, $N_{\text{jets}} \geq 1$, $N_{\text{jets}} \geq 2$, $N_{\text{jets}} \geq 3$ and VBF-enhanced fiducial regions, and cross-section limits at 95% confidence level in the single-lepton and high-$E_{\text{T}}^{\text{miss}}$ fiducial regions. The seven phase space regions are defined in section 3.

Fiducial region	Theoretical prediction (fb)	Source
Baseline	30.5 ± 3.3	LHC-XS [57] + XH
	$34.1\,^{+3.6}_{-3.5}$	STWZ [99] + XH
	$27.2\,^{+3.6}_{-3.2}$	HRES [103] + XH
$N_{\text{jets}} \geq 1$	13.8 ± 1.7	BLPTW [106] + XH
	$11.7\,^{+2.0}_{-2.4}$	JetVHeto [107] + XH
	$9.3\,^{+1.8}_{-1.2}$	MINLO HJ + XH
$N_{\text{jets}} \geq 2$	5.65 ± 0.87	BLPTW + XH
	$3.99\,^{+0.56}_{-0.59}$	MINLO HJJ + XH
$N_{\text{jets}} \geq 3$	0.94 ± 0.15	MINLO HJJ + XH
VBF-enhanced	0.87 ± 0.08	MINLO HJJ + XH
$N_{\text{leptons}} \geq 1$	0.27 ± 0.02	XH
$E_{\text{T}}^{\text{miss}} > 80$ GeV	0.14 ± 0.01	XH

Table 4. Theoretical predictions for the cross sections in the baseline, $N_{\text{jets}} \geq 1$, $N_{\text{jets}} \geq 2$, $N_{\text{jets}} \geq 3$, VBF-enhanced, single-lepton and high-$E_{\text{T}}^{\text{miss}}$ fiducial regions. The uncertainties on the cross-section predictions are discussed in detail in Section 8 and include the effect of scale and PDF variation as well as the uncertainties on the $H \to \gamma\gamma$ branching ratio and non-perturbative modelling factors. The seven phase space regions are defined in section 3. The 'XH' refers to the theoretical predictions for VBF, VH and $t\bar{t}H$ derived using the POWHEG-PYTHIA, and PYTHIA8 event generators discussed in section 4.

H→ γγ fiducial differential cross sections

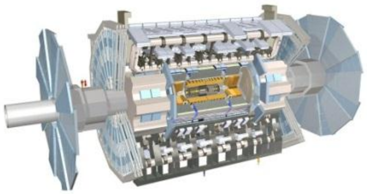

JHEP09(2014)112

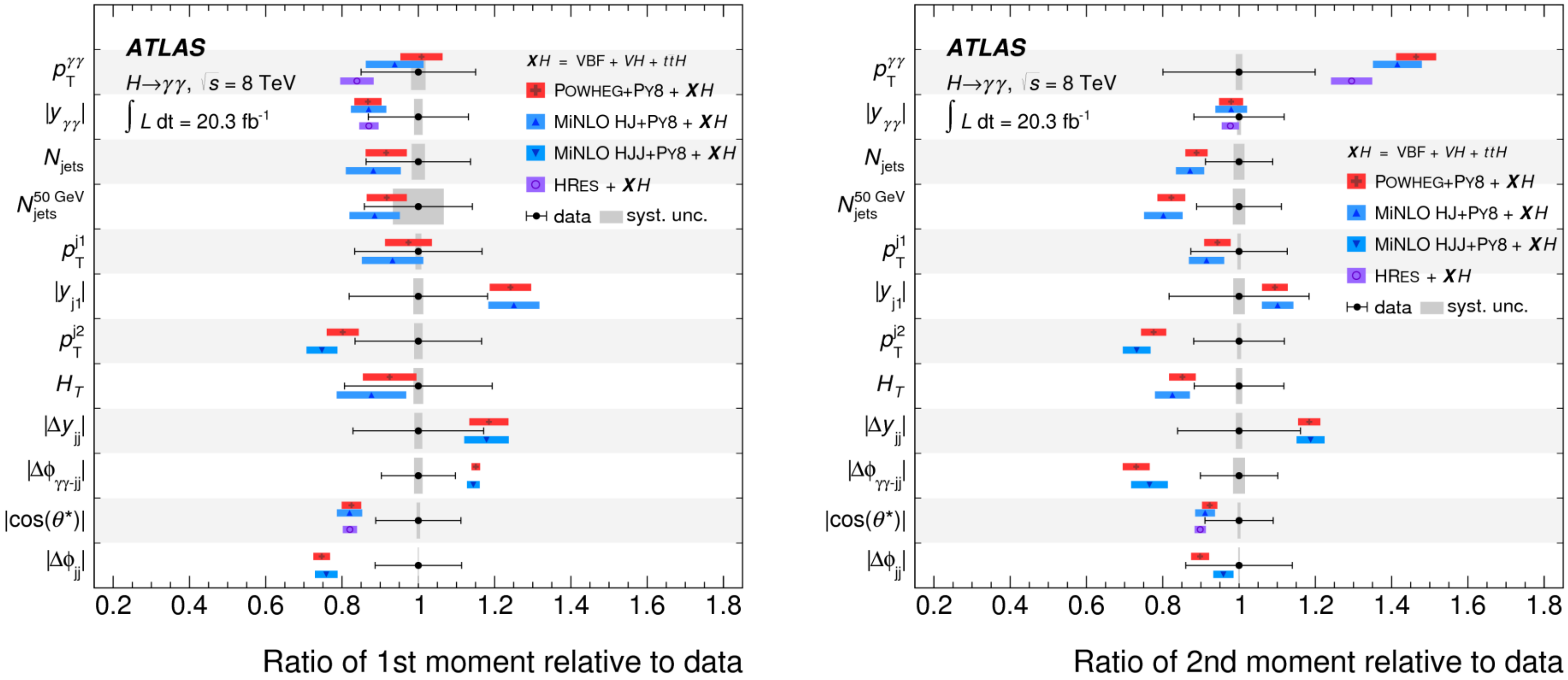

First and second moments of the differential distributions under study.

H→ γγ fiducial differential cross sections

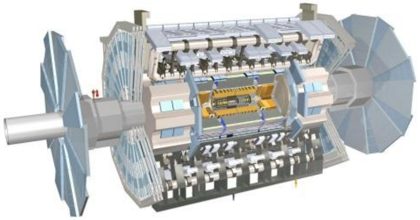

JHEP09(2014)112

Variable	POWHEG	MINLO HJ	MINLO HJJ	HRES
$p_{\mathrm{T}}^{\gamma\gamma}$	0.12	0.10	0.09	0.12
$\lvert y_{\gamma\gamma}\rvert$	0.81	0.83	0.83	0.80
$\lvert\cos\theta^{*}\rvert$	0.59	0.57	0.58	0.56
N_{jets}	0.42	0.36	0.30	-
$N_{\mathrm{jets}}^{50\ \mathrm{GeV}}$	0.33	0.33	0.30	-
H_{T}	0.43	0.39	0.34	-
$p_{\mathrm{T}}^{j_1}$	0.84	0.82	0.79	-
$\lvert y_{j_1}\rvert$	0.64	0.58	0.51	-
$p_{\mathrm{T}}^{j_2}$	0.34	0.29	0.23	-
$\lvert\Delta\phi_{jj}\rvert$	0.21	0.28	0.24	-
$\lvert\Delta y_{jj}\rvert$	0.64	0.58	0.49	-
$\lvert\Delta\phi_{\gamma\gamma,jj}\rvert$	0.45	0.46	0.42	-

Table 5. Probabilities from χ^2 tests for the agreement between the differential cross section measurements and the theoretical predictions. Each prediction is normalised to the LHC-XS cross section before selection.

H→ γγ fiducial differential cross sections

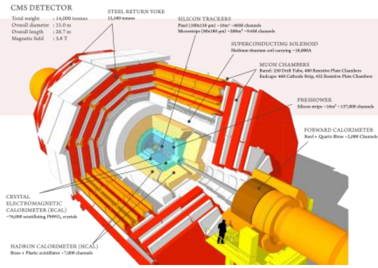

[CMS HIG-14-013]

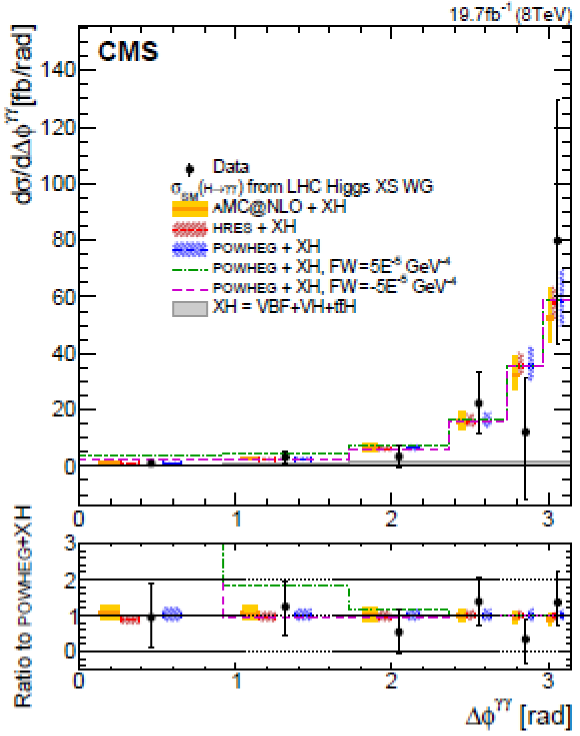

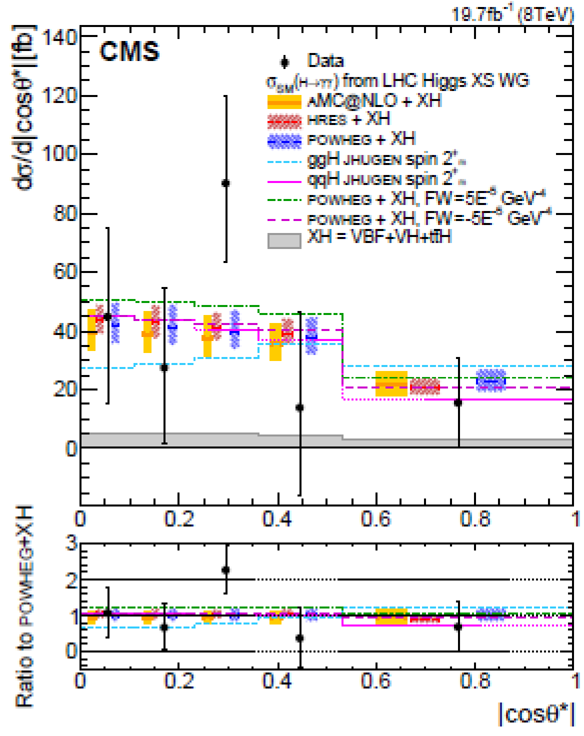

H→ γγ fiducial differential cross sections

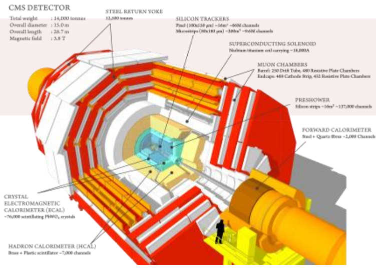

[CMS HIG-14-013]

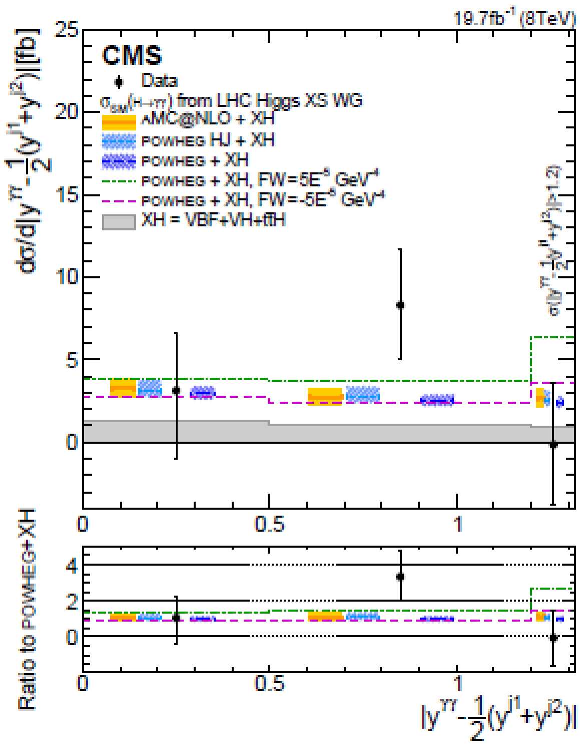

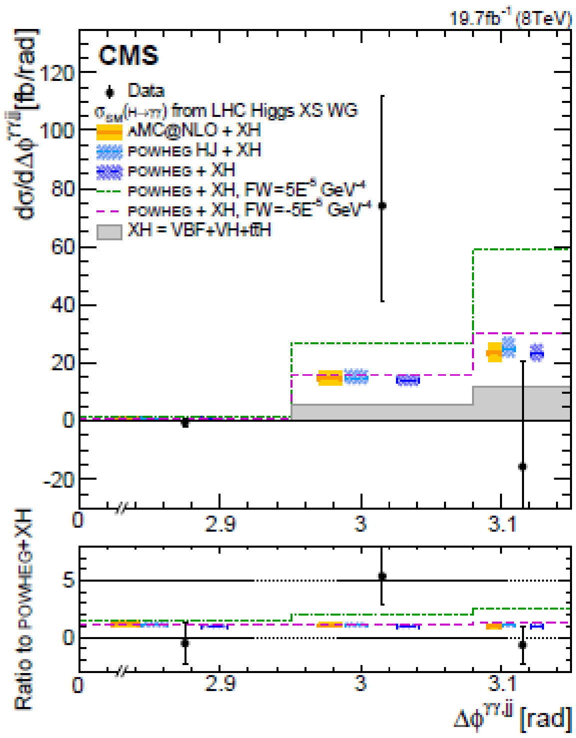

H→ γγ fiducial differential cross sections

ATLAS HIG-15-03, submitted to JHEP

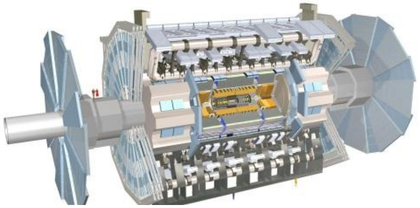

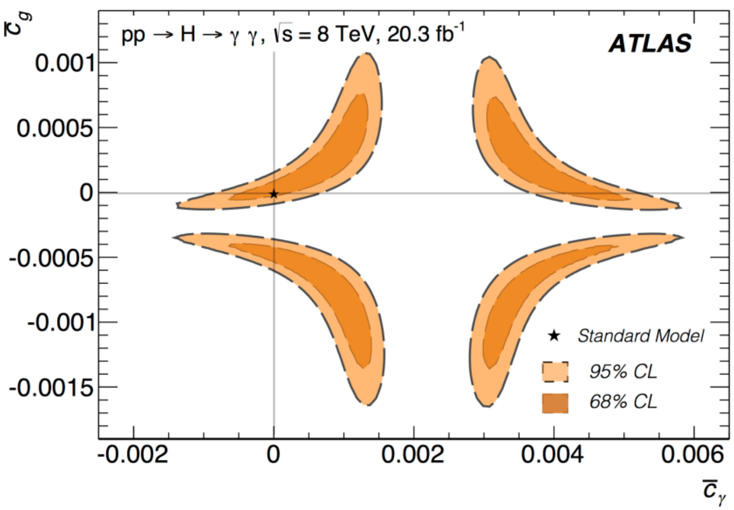

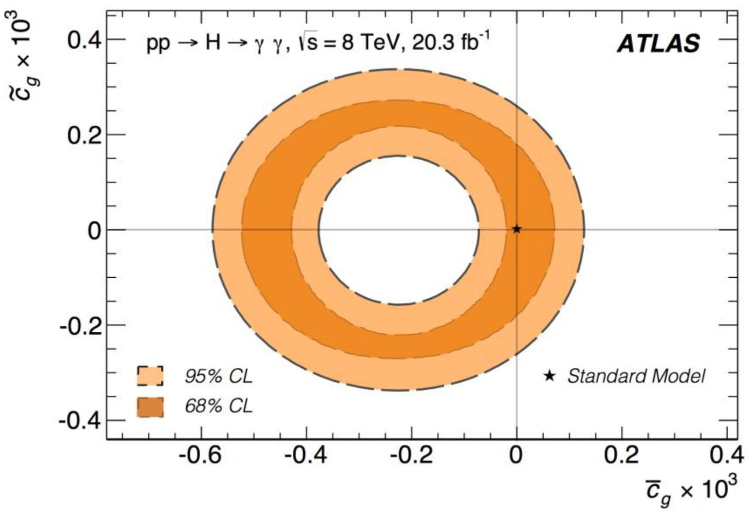

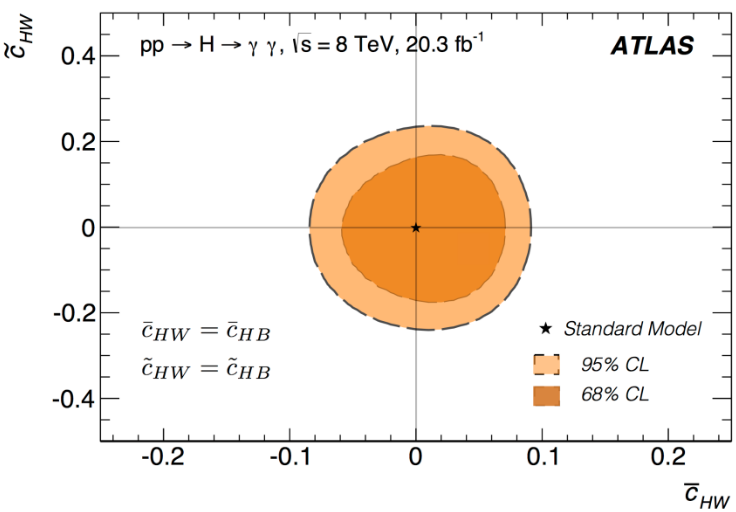

H→ ZZ(*)→4l fiducial differential cross sections

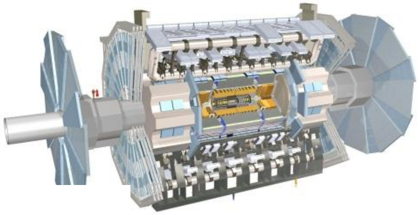

[Physics Letters B 738 (2014) 234-253]

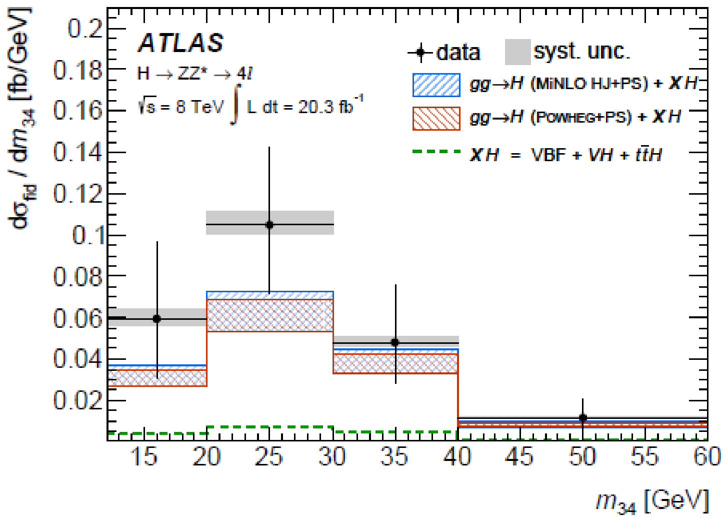

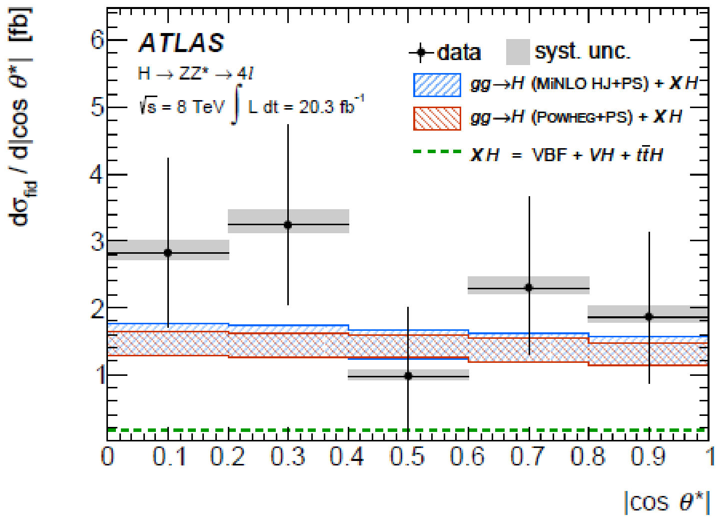

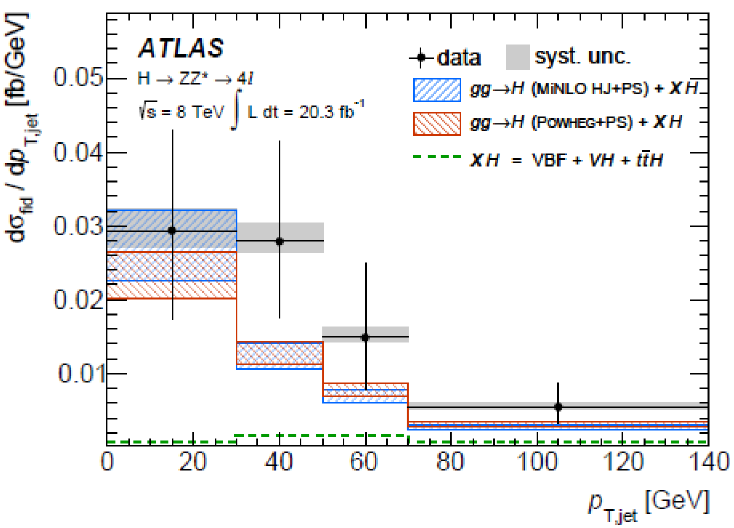

H→ γγ fiducial differential cross sections

P_T^H y^H N_{jets}

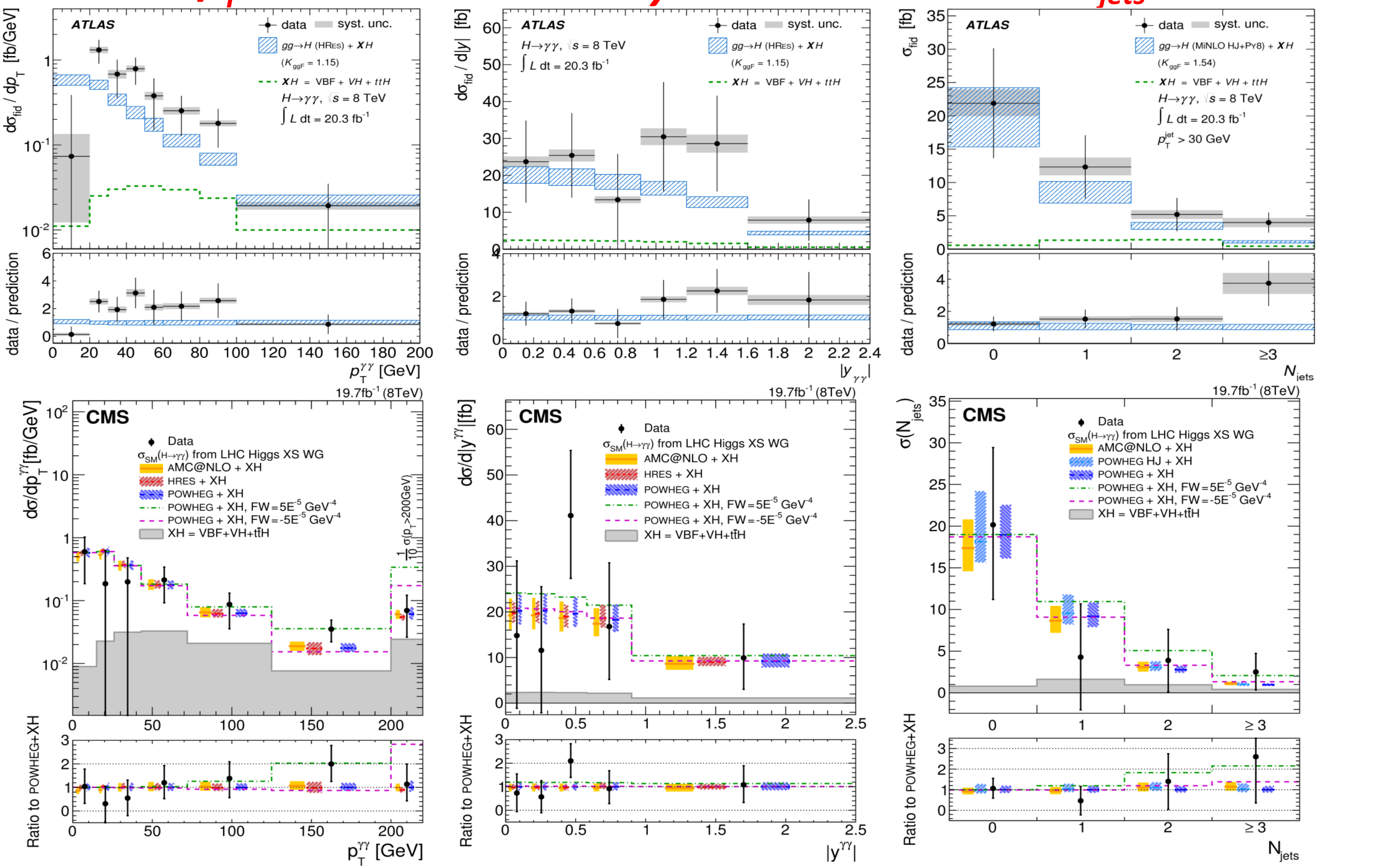

H→ γγ fiducial differential cross sections

P_T^{J1}

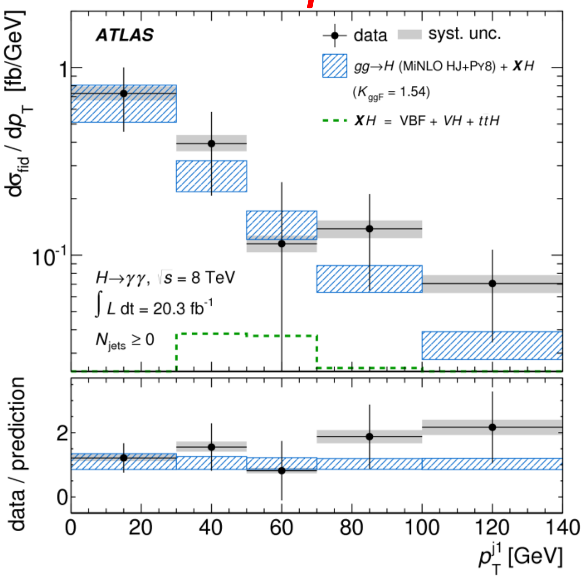

$\Delta\varphi^{jj}$

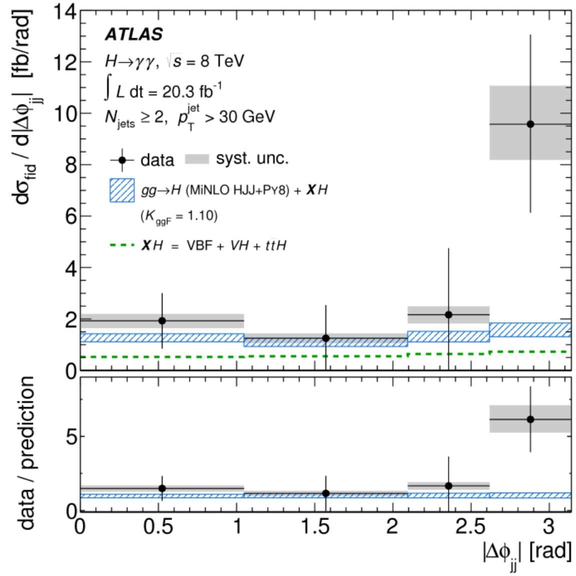

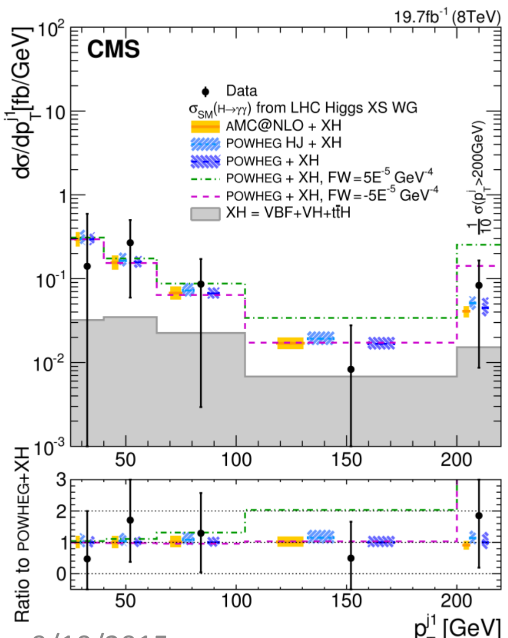

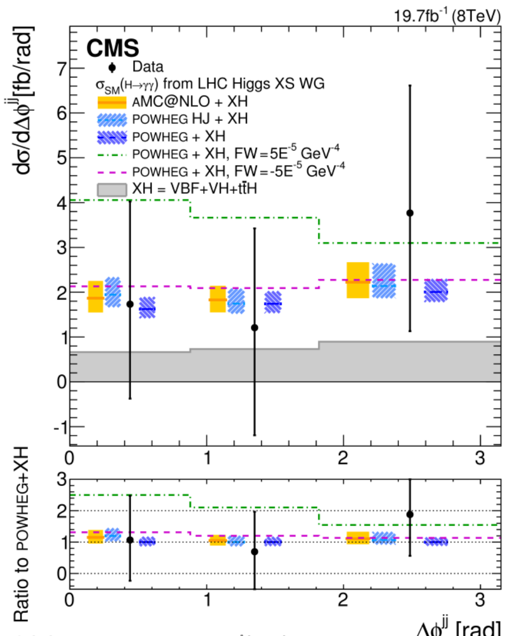

H→ ZZ(*)→4l fiducial differential cross sections

P_T^H

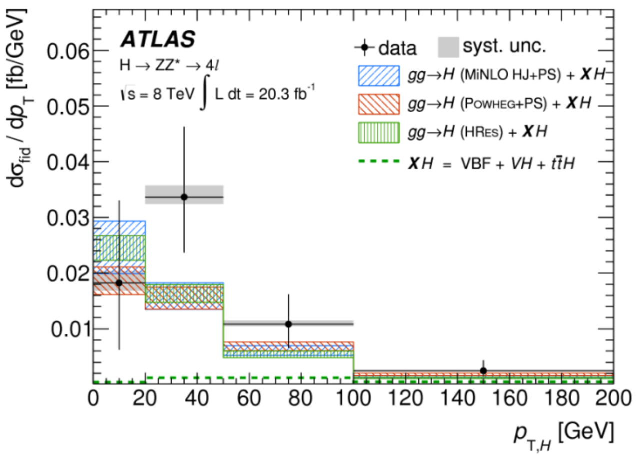

y^H

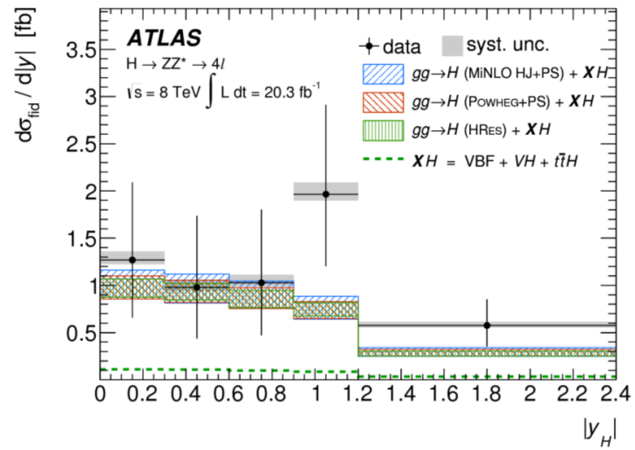

N_{jets}

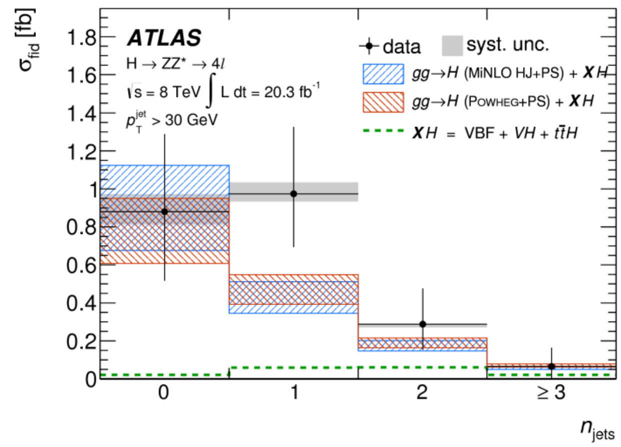

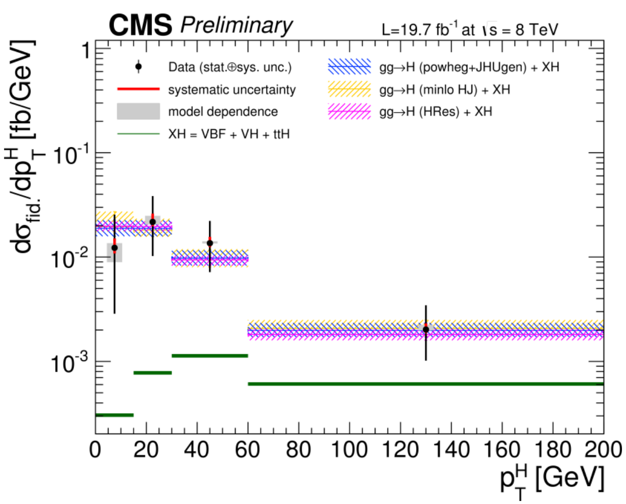

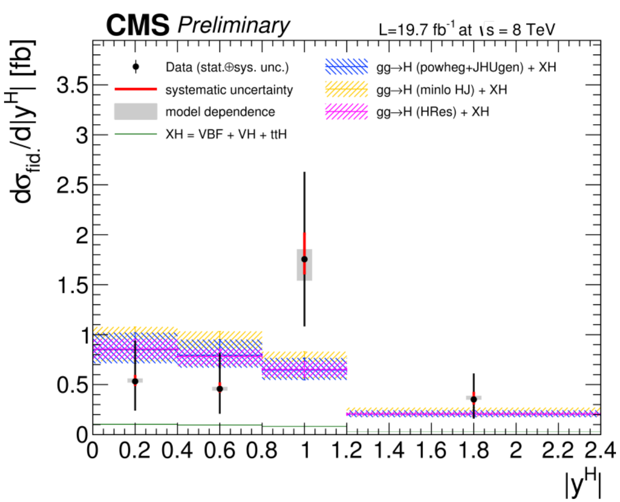

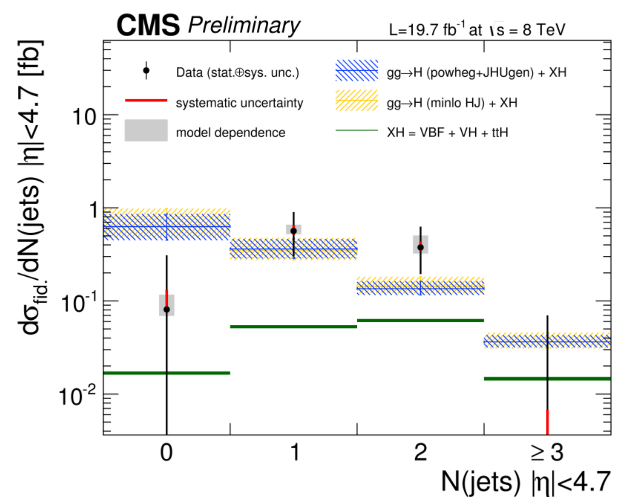

Inclusive cross section calculations

Inclusive **ggF** cross section calculations

LHC-XS	NNLO+NNLL[a,b,c]	CERN-2011-002(2011), arXiv1101.0593
ADDFGHLM	N^3LO[a,b,c]	J. High Energy Phys. 12 (2011) 058 - arXiv1503.6056
ABNY	NNLO+NNLL[a,b,c,d,e]	Phys. Lett. B 698 (2011) 271-274, arXiv1008.3162
STWZ	NNLO[c,d]	Phys. Rev. D 89 (2014) 054001, arXiv1307.1808
dFMMV	approx. N^3LO[c]	J. High Energy Phys. 10 (2014) 176, arXiv1408.6227
BBFMR	approx. N^3LO+N^3LL[a,b,c]	J. High Energy Phys. 09 (2014) 007, arXiv1405.3654

a Considers b- (and c-) quark masses in the $gg \to H$ loop
b Includes electroweak corrections
c Based on MSTW2008nnlo (α_s from PDF set)
d Uses π^2-resummed $gg \to H$ form factor
e Based on alternative counting, the result has N^3LL accuracy

Inclusive cross section calculations for additional production mechanisms

VBF : NNLO in QCD, NLO in EW
VH : NNLO in QCD, NLO in EW
ttH : NLO in QCD, LO in EW

Differential ggF cross section predictions

Analytical differential cross-section predictions		
HRes 2.2	NNLO+NNLL [a,e,f]	J. High Energy Phys. 09 (2013) 129, arXiv1306.4581
STWZ, BLPTW	NNLO+NNLL [c,d,e,g,h]	Phys. Rev. D 89 (2014) 074044, arXiv1312.4535
JetVHeto 2.0	NNLO+NNLL [a,c,e]	J. High Energy Phys. 01 (2014) 097, arXiv1308.4634
Monte Carlo event generators		
SHERPA 2.1.1	$H + 0, 1, 2$ jets @NLO [i,j]	Phys. Rev. D 90 (2014) 014012, arXiv1401.7971
MG5_aMC@NLO	$H + 0, 1, 2$ jets @NLO [i,k,l]	J. High Energy Phys. 07 (2014) 079, arXiv1405.0301
Powheg Nnlops	$\mathrm{NNLO}_{\geq 0j}$, $\mathrm{NLO}_{\geq 1j}$ [e,l,m]	J. High Energy Phys. 10 (2013) 222, arXiv1309.0017

a Considers b- (and c-) quark masses in the $gg \to H$ loop
b Includes electroweak corrections
c Based on MSTW2008nnlo (α_s from PDF set)
d Uses π^2-resummed $gg \to H$ form factor
e NNLO refers to the total cross section
f Based on the CT10nnlo PDF set
g This corresponds to NNLL′
h Includes 1-jet resummation included at NLL′+NLO
i Based on the CT10nlo PDF set
j Uses MEPS@NLO method and CKKW merging scheme
k Software version 2.2.1, NLO merged using FxFx scheme
l Interfaced with Pythia8 for parton showering
m Uses Minlo method & y^{H} reweighting to HNNLO.